Okamura N, Shiga Y, Furumoto S, Tashiro M, Tsuboi Y, Furukawa K, Yanai K, Iwata R, Arai H, Kudo Y, Itoyama Y, Doh-Ura K.	In vivo detection of prion amyloid plaques using [^{11}C]BF-227 PET.	Eur J Nucl Med Mol Imaging.	37	934-941	2010
Furukawa K, Okamura N, Tashiro M, Waragai M, Furumoto S, Iwata R, Yanai K, Kudo Y, Arai H.	Amyloid PET in mild cognitive impairment and Alzheimer's disease with BF-227: comparison to FDG-PET.	J Neurol.	257	721-727	2010
Shao H, Okamura N, Sugi K, Furumoto S, Furukawa K, Tashiro M, Iwata R, Matsuda H, Kudo Y, Arai H, Fukuda H, Yanai K.	Voxel-based analysis of amyloid positron emission tomography probe [^{11}C]BF-227 uptake in mild cognitive impairment and Alzheimer's disease.	Dement Geriatr Cogn Disord.	30	101-111	2010
Kikuchi A, Takeda A, Okamura N, Tashiro M, Hasegawa T, Furumoto S, Kobayashi M, Sugeno N, Baba T, Miki Y, Mori F, Wakabayashi K, Funaki Y, Iwata R, Takahashi S, Fukuda H, Arai H, Kudo Y, Yanai K, Itoyama Y.	In vivo visualization of alpha-synuclein deposition by carbon-11-labelled 2-[2-(2-dimethylaminothiazol-5-yl)ethenyl]-6-[2-(fluoro)ethoxy]benzoxazole positron emission tomography in multiple system atrophy.	Brain	133	1772-1778	2010
Watanuki S, Tashiro M, Miyake M, Ishikawa Y, Itoh M, Yanai K, Sakemi Y, Fukuda H, Ishii K.	Long-term performance evaluation of positron emission tomography: analysis and proposal of a maintenance protocol for long-term utilization.	Ann Nucl Med.	24	461-468	2010
Hayashi A, Abe N, Ueno A, Shigemune Y, Mori E, Tashiro M, Fujii T.	Neural correlates of forgiveness for moral transgressions involving deception.	Brain Res.	1332	90-99	2010
Abe N, Fujii T, Ueno A, Shigemune Y, Suzuki M, Tashiro M, Mori E.	Right temporal-lobe contribution to the retrieval of family relationships in person identification.	Neurosci Lett.	486	10-13	2010
Shigemune Y, Abe N, Suzuki M, Ueno A, Mori E, Tashiro M, Itoh M, Fujii T.	Effects of emotion and reward motivation on neural correlates of episodic memory encoding: a PET study.	Neurosci Res.	67	72-79	2010
Masud M, Fujimoto T, Watanuki S, Miyake M, Itoh M, Tashiro M.	Application of Positron Emission Tomography (PET) in Physical Medicine.	Mymensingh Med J.	19	110-115	2010
Omi R, Sano H, Ohnuma M, Kishimoto KN, Watanuki S, Tashiro M, Itoi E.	Function of the shoulder muscles during arm elevation: an assessment using positron emission tomography.	J Anat.	216	643-649	2010
Zhang D, Tashiro M, Shibuya K, Okamura N, Funaki Y, Yoshikawa T, Kato M, Yanai K.	Next-day residual sedative effect after nighttime administration of an over-the-counter antihistamine sleep aid, diphenhydramine, measured by positron emission tomography.	JClin Psychopharmacol.	30	694-701	2010
Kobayashi S, Abe Y, Tashiro M, Koike T, Iijima K, Imatani A, Ohara S, Watanabe S, Fukudo S, Shimosegawa T.	Brain activity following esophageal acid infusion using positron emission tomography.	World J. astroenterol.	16	5481-5489	2010
Nakamura K, Sekine Y, Ouchi Y, Tsujii M Yoshikawa E, Futatsubashi M, Tsuchiya KJ, Sugihara G, Iwata Y, Suzuki K, Matsuzaki H, Sugiyama T, Takei N, Mori N.	Brain serotonin and dopamine transporter bindings in adults with high-functioning autism	Arch Gen Psychiatry	67	59-68	2010
Yagi S, Yoshikawa E, Futatsubashi M, Yokokura M, Yoshihara Y, Torizuka T, Ouchi Y.	Progression from unilateral to bilateral parkinsonism in early Parkinsondisease: implication of mesocortical dopamine dysfunction by PET.	J Nucl Med.	51	1250-7	2010
Kono S, Ouchi Y, Terada T, Ida H, Suzuki M, Miyajima H.	Functional brainimaging in glucocerebrosidase mutation carriers with and without Parkinsonism.	Mov Disord.	25	1823-9	2010

Tajima S, Yamamoto S, Tanaka M, Kataoka Y, Iwase M, Yoshikawa E, Okada H, Onoe H, Tsukada H, Kuratsune H, Ouchi Y, Watanabe Y.	Medial Orbitofrontal Cortex Is Associated with Fatigue Sensation.	Neurology Research International	671421	1-5	2010
Kataoka K, hashimoto H, Kawabe J, Higashiyama S, Akiyama H, Shimada A, Kai T, Inoue K, Shiomi S, Kiriike N.	Frontal hypoperfusion in depressed patients with dementia of Alzheimer type demonstrated on 3DSRT	Psychiat Clin Neuros	64	293-298	2010

2. 英文総説

著者名	論文題名	雑誌名	巻	頁	出版年
Shinotoh H, Hirano S.	Emerging in vivo evidence of subcortical cholinergic dysfunction in Parkinsonian syndromes.	Neurology	74(18)	1406-7	2010

3. 英文単行本

著者名	論文題名	書名	編集者名	出版社名	出版地	頁	出版年
Tashiro M, Okamura N, Watanuki S, Furumoto S, Furukawa K, Funaki Y, Iwata R, Kudo Y, Arai H, Watabe H, Yanai K.	Quantitative Analysis of Amyloid β Deposition in Patients with Alzheimer's Disease Using Positron Emission Tomography.	Early Detection and Rehabilitation Technologies for Dementia: Neuroscience and Biomedical Applications	WU JINGLONG	IGI Global	Philadelphia, USA	in press	2011
Okamura N, Furumoto S, Tashiro M, Furukawa K, Arai H, Doh-ura K, Kudo Y, Yanai K.	Noninvasive Detection of Misfolded Proteins in the Brain Using [^{11}C]BF-227 PET	Early Detection and Rehabilitation Technologies for Dementia: Neuroscience and Biomedical Applications	WU JINGLONG	IGI Global	Philadelphia, USA	in press	2011

4. 邦文原著・症例報告

著者名	論文題名	雑誌名	巻	頁	出版年
片桐明，朝比奈正人，藤沼好克，赤荻悠一，山中義崇，福島剛志，篠遠仁，服部孝道，旭俊臣.	日本人健常高齢者における心拍変動に対する加齢と性差の影響	自律神経	47	381-385	2010

5. 邦文総説

著者名	論文題名	雑誌名	巻	頁	出版年
岩坪威、石井賢二	ADNIとアミロイドイメージング	Cognition and Dementia	9(4)	306-309	2010
石井賢二	アルツハイマー病患者と健常者におけるアミロイドイメージング	Cognition and Dementia	9(4)	293-300	2010
石井賢二	アルツハイマー病研究におけるアミロイドPET	BRAIN and NERVE	62(7)	757-767	2010
石井賢二	アルツハイマー病-update　臨床検査SPECT, PET	Clinical Neuroscience	28(9)	1015-1017	2010
石井賢二	日本でのアルツハイマー病研究の動き～J-ADNIにおけるPET検査の重要性と今後の展望～	Medical Now	67	6-9	2010

石井賢二	PETによるアミロイドイメージングの現状と展望	INNERVISION	26(1)	46-49	2011
齊藤祐子、初田裕幸、石井賢二、金丸和富、村山繁雄	高齢者におけるアミロイド蓄積の意義	Cognition and Dementia	10(1)	13-17	2011
石井賢二	アミロイドイメージングによる無症候性アミロイド陽性者の検出とその臨床的意義・問題点	Cognition and Dementia	10(1)	18-24	2011
石井賢二	PETによるアミロイドイメージングを用いたAD診断	MEDICAL IMAGING TECHNOLOGY	28(1)	26-30	2010
篠遠 仁	認知症の診断-この10年とこれから- 機能画像の進歩	老年精神	21	42-48	2010
篠遠 仁	認知症でみられる非認知症状とその対応. 3)代表的な身体合併症	神経内科	72 [Suppl.6]	151-156	2010
島田 斉, 樋口 真人	アミロイドとミクログリアの画像化	Frontiers in Parkinson Disease	第3巻第4号	32-35	2010
島田斉, 伊藤彰一	Voxel-based morphometry	Clinical Neuroscience	28	527-530	2010
伊藤健吾, 加藤隆司	Alzheimer病 6）画像診断－PETによる早期および鑑別診断のエビデンスと臨床研究－	神経内科	72 [Suppl.6]	290-295	2010
伊藤健吾, 加藤隆司	アルツハイマー病のFDG PETコホートの現状	PETジャーナル	11	32-34	2010
百瀬敏光	認知症診療における画像診断の役割と可能性－放射線科医の立場から－	Innervision	26(1)	6-9	2011
高橋美和子, 百瀬敏光	SPECT －主に血流評価による早期診断と鑑別診断を中心に（心交感神経シンチグラフィーを含む）	Innervision	26(1)	21-24	2011

6. 邦文単行本

著者名	論文題名	書名	編集者名	出版社名	出版地	頁	出版年
石井賢二	アルツハイマー病の発症はアミロイドイメージングでどこまで予測できるか？	EBM精神疾患の治療2011-2012	上島国利, 三村將, 中込和幸, 平島奈津子	中外医学社	東京	241-246	2011
石井賢二	診断薬と診断補助薬, 診断用機器 ～脳アミロイド診断薬～	新薬展望2011（医薬ジャーナル増刊号）		医薬ジャーナル社	大阪	403-408	2011
石井賢二	アミロイドPET画像で診るアルツハイマー病	見て診て学ぶ認知症の画像診断. 改訂第2版	松田博史, 朝田隆	永井書店	東京	179-189	2010
石井賢二	認知症	臨床医とコメディカルのための最新クリニカルPET	米倉義晴ほか	先端医療技術研究所	東京	179-183	2010
石井賢二	認知症の画像所見 SPECT･PET	最新医学・別冊 新しい診断と治療のABC 66 認知症	三村将	最新医学社	東京	170-178	2010
篠遠 仁	アセチルコリンエステラーゼイメージング	見て診て学ぶ認知症の画像診断. 改訂第2版	松田博史, 朝田隆	永井書店	大阪	380-390	2010

Ⅳ. 研究成果の刊行物・別刷

OPEN ACCESS Freely available online

PLoS one

Binding of Pramipexole to Extrastriatal Dopamine D_2/D_3 Receptors in the Human Brain: A Positron Emission Tomography Study Using ^{11}C-FLB 457

Kenji Ishibashi[1,2]*, Kenji Ishii[1], Keiichi Oda[1], Hidehiro Mizusawa[2], Kiichi Ishiwata[1]

1 Positron Medical Center, Tokyo Metropolitan Institute of Gerontology, Tokyo, Japan, 2 Department of Neurology and Neurological Science, Graduate School, Tokyo Medical and Dental University, Tokyo, Japan

Abstract

The purpose of this study was to determine the binding sites of pramipexole in extrastriatal dopaminergic regions because its antidepressive effects have been speculated to occur by activating the dopamine D_2 receptor subfamily in extrastriatal areas. Dynamic positron emission tomography (PET) scanning using ^{11}C-FLB 457 for quantification of D_2/D_3 receptor subtype was performed on 15 healthy volunteers. Each subject underwent two PET scans before and after receiving a single dose of pramipexole (0, 0.125, or 0.25 mg). The study demonstrated that pramipexole significantly binds to D_2/D_3 receptors in the prefrontal cortex, amygdala, and medial and lateral thalamus at a dose of 0.25 mg. These regions have been indicated to have some relation to depression and may be part of the target sites where pramipexole exerts its antidepressive effects.

Citation: Ishibashi K, Ishii K, Oda K, Mizusawa H, Ishiwata K (2011) Binding of Pramipexole to Extrastriatal Dopamine D_2/D_3 Receptors in the Human Brain: A Positron Emission Tomography Study Using ^{11}C-FLB 457. PLoS ONE 6(3): e17723. doi:10.1371/journal.pone.0017723

Editor: Kenji Hashimoto, Chiba University Center for Forensic Mental Health, Japan

Received November 30, 2010; **Accepted** February 13, 2011; **Published** March 9, 2011

Funding: Funding for this work was supported by a Grant-in-Aid for Scientific Research (B) No. 20390334 (Ishiwata K) by the Japan Society for the Promotion of Science (JSPS). JSPS had no further role in study design, data collection and analysis, decision to publish, or preparation of the manuscript.

Competing Interests: The authors have declared that no competing interests exist.

* E-mail: kenji_ishibashi@pet.tmig.or.jp

Introduction

Pramipexole is a dopamine D_2 receptor (D_2R) subfamily agonist. It was introduced for treating motor symptoms in patients with idiopathic Parkinson's disease (PD) [1] and has been shown to be effective by various clinical trials [2,3]. In addition, various studies have recently found antidepressive effects of pramipexole not only in patients with PD complicated by depressive state [4,5,6,7], but also in depressive patients without parkinsonian symptoms [8,9,10,11,12,13,14,15,16]. Its antidepressive effects have been also shown in animal experiments [17,18].

The D_2R subfamily consists of D_2, D_3, and D_4 receptor subtypes [19]. Pramipexole is active mainly at D_2 and D_3 receptors, and compared with other dopamine agonists, it is unique in that the binding affinity for D_3 receptors is higher than that for D_2 receptors [20,21,22,23]. Kvernmo et al. reported that binding affinities (inhibition constant; K_i) for cloned human D_2 and D_3 receptors of pramipexole were 3.9 and 0.5 nmol/L, respectively [23]. The distribution of D_3 receptors in the brain is different from that of D_2 receptors [24,25,26,27,28,29]. Compared with D_2 receptors, D_3 receptors are predominantly located in extrastriatal regions including the mesolimbic dopamine system involved in mood and behavior. On the other hand, although both D_2 and D_3 receptors in the striatum are much more abundant than those in other regions, the D_2 receptor density is higher than the D_3 receptor density in the striatum. Stimulation of D_2 and D_3 receptors appears to induce different effects.

There are growing evidences that D_3 receptors may play a role in the pathogenesis of depression because of their pharmacology and distribution in the brain [26,30,31], although the exact mechanism remains unknown. The mechanism of antidepressive effects and extrastriatal binding sites of pramipexole are also unknown, and no study has investigated this issue. These effects have been speculated to occur by means of activation of D_2R subfamily, especially the D_3 receptor subtype, in the mesolimbic dopamine system [1]. Therefore, we aimed to determine the binding sites of pramipexole in the extrastriatal dopaminergic regions by using ^{11}C-FLB 457 positron emission tomography (PET) scanning for quantification of D_2/D_3 receptors in extrastriatal brain regions. In addition, we discussed whether the regional sites occupied by pramipexole may be target sites where pramipexole exerts its antidepressive effects on the basis of previous anatomical and functional reports on depression.

Materials and Methods

Subjects

This study protocol was approved by the Ethics Committee of the Tokyo Metropolitan Institute of Gerontology. Written informed consent was obtained from all participants. A total of 15 healthy volunteers (7 men and 8 women; mean age = 50.2 years, SD = 11.7, range = 30–77) participated in the study. All subjects underwent two ^{11}C-FLB 457 PET scans and magnetic resonance imaging (MRI) of the brain. They were classified into 3 groups according to the dose of pramipexole (0.25, 0.125, or 0 mg). The 5 subjects in the high-dose group (2 men and 3 women, 57.2±12.8 years) received a single oral 0.25 mg dose of pramipexole. Another 5 subjects in the low-dose group (2 men and 3 women, 51.4±9.4 years) received a single oral 0.125 mg dose of pramipexole. The drug was administered between the two PET

scans. The other 5 subjects were in the control group (3 men and 2 women, 42.0±6.3 years) and received no medication. Significant difference was not found in age between the 3 groups with one-way ANOVA test. All volunteers were free of any current or past mental disorders, and defined as healthy on the basis of their medical history, the results of their physical and neurological examinations and routine mental health interview performed by a neurologist, and the findings of the MRI. None had been receiving any other medications at the time of this study.

Doses of pramipexole

Previous studies have shown that administration of more than approximately 1 mg of pramipexole exerts antidepressive effects [4,5,6,7,8,9,10,11,12,13,14,15,16]; compared with these studies, the doses of pramipexole used in our study were low. We chose these low doses to ensure the safety of the participants in this study.

According to unpublished data on file in Nippon Boehringer Ingelheim (Tokyo, Japan), a single administration of pramipexole 0.4 mg caused orthostatic hypotension in an early clinical trial of German volunteers. On the basis of these results, the doses of pramipexole were set at 0.1, 0.2, and 0.3 mg in the Phase one clinical trial of Japanese volunteers, and no one developed more than moderate adverse effects. After oral administration of a single dose of pramipexole 0.1 mg, C_{max}, T_{max}, and $t_{1/2}$ were 294.6±46.3 pg/mL, 1.5±0.5 h and 7.71±1.90 h (mean ± SD), respectively. After administration of pramipexole 0.2 mg, the values were 583.2±69.9 pg/mL, 1.4±0.5 h, and 6.36±1.46 h, respectively; after a dose of 0.3 mg, the values were 766.3±88.8 pg/mL, 2.3±1.2 h, and 6.94±1.09 h, respectively. One tablet of pramipexole equals 0.125 mg. Therefore, the doses of pramipexole were set at 0.25 and 0.125 mg in this study.

^{11}C-FLB 457 PET imaging

Each volunteer participated in two ^{11}C-FLB 457 PET scans on the same day—one in the morning and another in the afternoon. Of 15 subjects, 10 were administered with either 0.25 or 0.125 mg of pramipexole after the first PET scan; the second PET scan took place 1–1.5 h later because the concentration of pramipexole in plasma reaches its peak in approximately 1–2 hours as described above.

PET imaging was performed at the Positron Medical Center, Tokyo Metropolitan Institute of Gerontology, with a SET-2400W scanner (Shimadzu, Kyoto, Japan). The spatial resolution was 4.4 mm full width at half maximum in the transverse direction and 6.5 mm full width at half maximum in the axial direction. Images with 50 slices were obtained with a 2×2×3.125-mm voxel size and a 128×128 matrix size. The transmission data were acquired by using a rotating ^{68}Ga/^{68}Ge rod as a source for attenuation correction. ^{11}C-FLB 457 was prepared as described previously [32].

In the first PET experiment, the injected dose, specific activity, and mass of injected ligand were 283±24 MBq, 118±45 GBq/μmol, and 3.0±1.7 μg (mean ± SD), respectively. The respective values in the second PET experiment were 285±19 MBq, 110±38 GBq/μmol, and 3.2±2.0 μg. The time interval between the first and second injections of ^{11}C-FLB 457 was 4–4.5 hours. The mass of injected ligand in each second scan was carefully adjusted to that in each first scan because of potential occupancy effects by unlabelled ligand itself [33,34], and no significant difference was found in the mass of injected ligand as well as the injected dose and specific activity between the first and second scans in each group, using paired Student *t* test.

A dynamic series of decay-corrected PET data acquisition was performed in the 3D mode for 90 minutes starting at the time of the intravenous injection of ^{11}C-FLB 457. The frame arrangement was 20 s ×6 frames, 60 s ×2 frames, 180 s ×2 frames, and 300 s ×16 frames.

For the 5 subjects in the high-dose group, arterial blood samples were also obtained. Immediately after the intravenous injection of ^{11}C-FLB 457, 18 arterial blood samples were collected at 10-s intervals over 3 min; the next 2 samples were collected at 60-s intervals over 2 min, and the remaining 10 samples were collected at longer intervals, for a total of 30 samples. All samples were manually drawn. Plasma was separated, weighed, and measured for radioactivity with a sodium iodide (TI) well scintillation counter. Six samples collected at 3, 10, 20, 30, 40, and 60 minutes were further processed by high-performance liquid chromatography to determine the fractions of plasma radioactivity corresponding to unchanged ^{11}C-FLB 457 and labeled metabolites, as described previously [32].

Data analysis

Image manipulations were performed using Dr. View version R2.0 (AJS, Tokyo, Japan) and statistical parametric mapping 2 (SPM2; Functional Imaging Laboratory, London, UK) implemented in MATLAB version 7.0.1 (The MathWorks, Natick, MA). First, individual two dynamic ^{11}C-FLB 457 images and MRI images were coregistered. Next, regions of interest (ROIs) were defined over the prefrontal, parietal, lateral temporal and anterior cingulate cortices, medial and lateral parts of the thalamus, amygdala, hippocampus, and cerebellum on the individual coregistered MRI. These ROIs were spatially moved on the corresponding coregistered dynamic ^{11}C-FLB 457 images.

^{11}C-FLB 457 binding to extrastriatal D_2/D_3 receptors was calculated as the binding potential (BP) by the simplified reference tissue model (SRTM) using cerebellum as a reference tissue [35]. BP derived with this method is referred to as BP_{ND_SRTM} (ND: nondisplaceable). For the high-dose group with arterial blood samples, the binding was also analyzed by using the linear graphic analysis by Logan et al. [36]. The slope of the linear phase of the obtained plot corresponds to the total distribution volume (V_T) of the ligand plus the plasma volume. The regional V_T was determined from the slope, and the BP with this method was calculated as follows using cerebellum as a reference region: BP_{ND_Logan} = (V_T on ROI/V_T on cerebellum) - 1.

D_2/D_3 occupancy rate by pramipexole was calculated for each ROI by using the following equation: occupancy rate (%) = 100× (BP at baseline – BP at pramipexole-loading)/BP at baseline. BP at baseline and BP at pramipexole-loading are obtained from first and second PET scans, respectively. Data were expressed as mean ± SD.

Statistical Analysis

The differences between first and second PET scans were tested by paired Student's *t*-test. Correlations between BP_{ND_SRTM} and BP_{ND_Logan} in high-dose group were assessed by means of linear regression analysis with Pearson's correlation test. P values<0.05 were considered statistically significant.

Results

For the high-dose group, BP_{ND_SRTM} was found to be significantly correlated with BP_{ND_Logan} ($r = 0.97$; $P<0.01$) using data of both the first and second experiments, as shown in Figure 1. Although the slope of the regression line was slightly less than one, the BP_{ND_SRTM} and BP_{ND_Logan} had almost a one-to-one relationship.

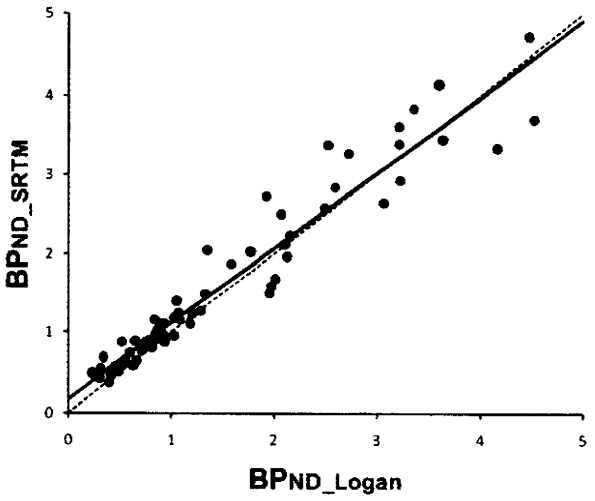

Figure 1. Correlation between BP_{ND_Logan} and BP_{ND_SRTM}. The binding potential estimated by Logan plot method and that estimated by the simplified reference tissue model method are represented as BP_{ND_Logan} and BP_{ND_SRTM}, respectively. The solid line represents the regression line. Linear correlation is significant ($r = 0.97$, $P < 0.01$, $y = 0.95x + 0.17$). The dotted line represents the line of "y = x" for reference. ND: nondisplaceable.
doi:10.1371/journal.pone.0017723.g001

Each regional BP_{ND} of first and second PET scans for each dose of pramipexole is shown in Figure 2. After administration of pramipexole 0.25 mg, BP_{ND_Logan} in the prefrontal cortex ($P = 0.03$, $t = 3.15$), medial ($P = 0.01$, $t = 4.56$) and lateral ($P = 0.01$, $t = 3.78$) thalamus, and amygdala ($P = 0.02$, $t = 3.32$) and BP_{ND_SRTM} in medial ($P = 0.01$, $t = 4.51$) and lateral ($P = 0.02$, $t = 3.33$) thalamus decreased significantly. D_2/D_3 occupancy rates estimated with BP_{ND_Logan} in the prefrontal cortex, medial and lateral thalamus, and amygdala were 10.3%±6.8%, 16.7%±6.9%, 14.9%±8.9%, and 20.4%±8.6%, respectively. Occupancy rates estimated with BP_{ND_SRTM} in the medial and lateral thalamus were 10.3%±5.0% and 10.8%±6.4%, respectively. No significant difference was found in occupancy rates estimated with either BP_{ND_Logan} or BP_{ND_SRTM} between the medial and lateral thalamus, using paired Student t test. In the low-dose group with 0.125 mg of pramipexole and in the control group, there was no significant correlation between BP_{ND_SRTM} of the two PET scans in all regions.

The time-activity curves of representative regions before and after administration of pramipexole 0.25 mg are displayed in Figure 3. Visually, the radioactivity levels of the putamen, entire thalamus and amygdala seemed to decrease after administration of pramipexole 0.25 mg. On the other hand, the radioactively level of the cerebellum seemed mostly unchanged between the first and second scans. Actually, V_T on the cerebellum estimated by Logan plot method in the first and second PET scans was 4.55±0.68 and 4.67±0.97, respectively, and no significant difference was found between the two.

Discussion

Pramipexole is a synthetic aminobenzothiazole derivative with selective actions mainly on D_2 and D_3 receptors, and it binds with the highest affinity to D_3 receptors [20,21,22,23]. In the brain, the distribution of D_3 receptors is known to be different from that of D_2 receptors [24,25,26,27,28,29], although there are some differences in the relative proportion of D_2 and D_3 receptors between the previous studies. The D_2 binding sites are widely detected with the highest concentration found in the striatum, followed by the nucleus accumbens, external segment of the globus pallidus, substantia nigra and ventral tegmental area. The distribution of D_3 receptors is relatively restricted and D_3 binding sites are enriched in the amygdala, nucleus accumbens, ventral

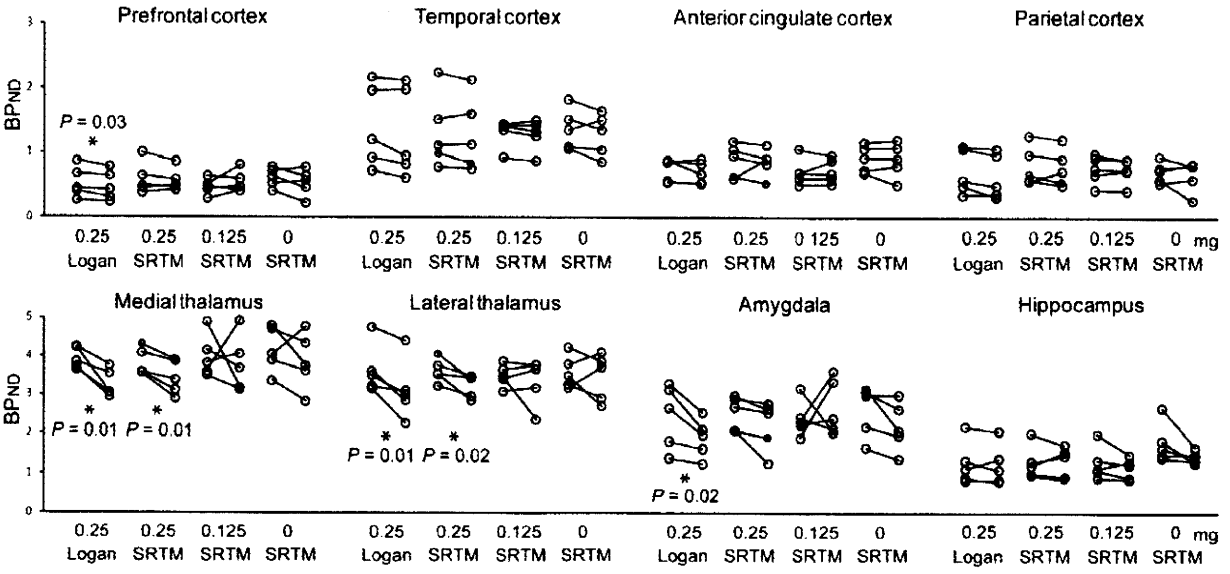

Figure 2. Changes in BP_{ND} between first and second PET scans in each extrastriatal region. For 0.25 mg dose group, each BP_{ND} was estimated by the Logan plot method and simplified reference tissue model method. For 0.125 mg and 0 mg dose groups, each BP_{ND} was estimated only by the simplified reference tissue model method. Pramipexole was orally administered 1–1.5 h before second PET scanning at doses of 0.25 mg, 0.125 mg. Each P value was estimated by paired Student's t-test between first and second PET scans. Significant differences were found only in the high-dose group (* $P < 0.05$). BP: binding potential, ND: nondisplaceable.
doi:10.1371/journal.pone.0017723.g002

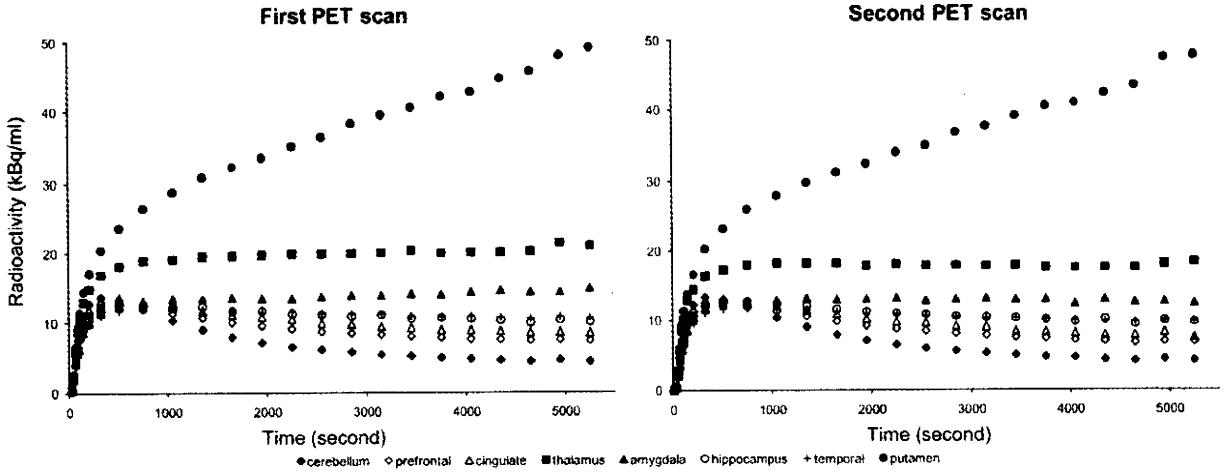

Figure 3. Average time-activity curves of representative regions of five subjects before (left) and after (right) administration of pramipexole 0.25 mg. Each point was normalized to the radioactivity of 185 MBq. The time-activity curve of the putamen is displayed for reference. Thalamus (■) represents the entire thalamus.
doi:10.1371/journal.pone.0017723.g003

striatum, substantia nigra, anteroventral nucleus of the thalamus and internal segment of the globus pallidus. Thus, D_2 or D_3 binding sites are located in the synapse of the afferent structures as well as the neurons of the efferent structures such as substantia nigra and ventral tegmental area. D_2 or D_3 receptors in the efferent structures are thought to act as autoreceptors, which could play an important role in regulating the activity of dopaminergic neurons [24,29].

On the other hand, in this study, the BP_{ND} in the substantia nigra or ventral tegmental area could not be quantified with reliability, because the structures were too small for usual ROI analysis of the dynamic data on the basis of the resolution of the PET scanner and the number of subjects was relatively small. For the same reasons, the ROIs were drawn over not each small nucleus but medial and lateral parts of the thalamus although the thalamus is known to have a great deal of regional heterogeneity in D_2 and D_3 expression. Also, the BP_{ND} in the striatal and its closely neighbor regions such as the ventral striatum and globus pallidus could not be quantified using ^{11}C-FLB 457 because a long time more than a few hours is needed for reaching equilibration in the striatum [37]. Based on the distribution of D_2 and D_3 receptors and the technical matters as described above, we investigated the binding sites of pramipexole especially in the limbic system, thalamus and cortical regions. To our knowledge, this is the first in vivo study that has investigated the relationship between a dopamine agonist and its binding sites in extrastriatal regions.

This study showed that a single dose of pramipexole 0.25 mg decreased BP_{ND_Logan} significantly in the prefrontal cortex, amygdala, and thalamus. The mesolimbic pathway begins in the ventral tegmental area of the midbrain and projects to the limbic areas, including the nucleus accumbens in the ventral striatum, amygdala, and hippocampus; it also projects to the cortical areas, including the prefrontal and cingulate cortices. The latter cortical pathway is called as the mesocortical pathway. Both pathways are known to be involved in the depressive state [38,39,40,41]. Indeed, the amygdala is important for emotional processing and its functional abnormalities are associated with depression [42,43,44], and frontal cortical dopamine function has been reported to be involved in depression [45,46,47]. In the mesolimbic pathway, D_2 and D_3 binding sites are predominant in the hippocampus and amygdala, respectively [24,25,27], and this difference may be one of the reasons that significant decrease of BP_{ND_Logan} was not found in the hippocampus. The mesocortical pathway also has D_3 receptors as well as D_2 receptors [27,29], although there is no detail report on the relative proportion of D_2 and D_3 receptors in that area. The thalamic dopaminergic system has been recently identified; this system is speculated to have a prominent role in depression, especially in regard to emotion, attention, cognition, and complex somatosensory and visual processing [44,48,49,50]. Although this study could not find the significant difference between medial and lateral parts of the thalamus, D_3 binding sites are relatively abundant and especially tend to be concentrated along the midline in the thalamus, while D_2 binding sites are more homogeneously distributed [24,27]. On the basis of the relationship between the occupied sites by pramipexole, the distribution of D_2 and D_3 receptors and previous anatomical and functional reports on depression, it is reasonable to suggest that pramipexole may exert its antidepressive effects by activating D_2R subfamily, especially the D_3 receptor subtype, in these regions (prefrontal cortex, amygdala, and thalamus).

With regard to the BP_{ND_SRTM} method, after administration of a single dose of pramipexole 0.25 mg, binding in the medial and lateral thalamus decreased significantly as shown in the BP_{ND_Logan} method, and bindings in both the prefrontal cortex and amygdala showed the tendency to decrease without significant difference. On the other hand, there was no significant difference between first and second PET scans in both the low-dose group and the control group. On the basis of the difference between the high-dose group and the other two groups, we speculate that the effects of pramipexole may be dose dependent, although it is impossible to confirm this finding only with our data. Despite the high correlation between BP_{ND_Logan} and BP_{ND_SRTM} methods as shown in Figure 1, the discrepancies between the both methods found in the high-dose group could be explained by the interindividual and intraindividual variability of each analytical method [51,52,53]. However, BP_{ND_Logan} estimated with artery blood samples should be regarded as more reliable and accurate than BP_{ND_SRTM} estimated without artery blood samples, and the findings for the prefrontal cortex and amygdala, where only the BP_{ND_Logan} method showed significance, were considered to be meaningful.

Vilkman et al. conducted a test-retest analysis of ^{11}C-FLB 457 PET scanning with 7 healthy volunteers (mean age ± SD = 29.0±6.9) and suggested that coefficient of variation (COV) of each extrastriatal region in BP_{ND_Logan} and BP_{ND_SRTM} methods was about 20% and the reproducibility of both methods was good [51]. Consistent with Vilkman et al., our results of the control group corresponding to a test-retest analysis showed no significant difference in BP_{ND_SRTM} of each region between first and second PET scans. In the control group, the COV of each region between the first and second experiments was similar, and the ranges of COV in the first and second experiments were 19.3%–33.9% and 16.3%–38.5%, respectively. Thus, the reproducibility of the BP_{ND_SRTM} method in this study was good. Compared with previous studies [51,52,53], the COV in our control group was somewhat larger. A possible explanation for this difference could be given by following two reasons. One is the relatively smaller number of subjects, and the other is the relatively larger variability in age because D_2R subfamily in each extrastriatal region is known to show age-related decline [54,55].

In vitro brain homogenate binding studies have demonstrated that D_2R subfamily exists in two affinity states, i.e., high and low affinity states [56,57,58]. The high affinity state is thought to represent the functional state, and agonists bind preferentially to D_2R subfamily in the high affinity state, while antagonists have equal affinity for D_2R subfamily in the high and low affinity states. In vivo competition studies between endogenous dopamine and a labeled agonist or antagonist ligand estimated the percentage of high affinity state to be about 60–70% [59,60]. On the other hand, some recent in vivo studies indicated that most D_2R subfamily is in the high affinity state at living conditions because the binding of exogenous unlabeled agonist to D_2R subfamily in high or low affinity states could not be differentiated with either a labeled agonist or antagonist ligand [61,62]. Thus, the accurate proportion of the two states remains controversial. In this study, relatively low D_2/D_3 occupancy rates by pramipexole were mainly due to low dose of pramipexole. However, based on the two states theory, another reason may be because D_2/D_3 occupancy rates by agonist pramipexole were estimated by antagonist ligand ^{11}C-FLB 457.

One of the drawbacks of this study may be that we used the cerebellum as a reference region, in order to gain smaller variability and better reproducibility for the analysis of the PET data, compared with the two-tissue compartment four-rate constant model [51]. Asselin et al. reported that using the cerebellum as a reference region could lead to underestimation of BP_{ND} and occupancy rate [63]. However, we showed no statistical difference in V_T on the cerebellum estimated by Logan plot method before and after administration of pramipexole 0.25 mg, and at least our data, especially in the high-dose group, would be appropriate for the purpose of confirming the extrastriatal effects of a dopamine agonist. Other drawbacks of this study may be that we collected arterial blood samples only from the high-dose group, the number of subjects was relatively small and a dose of pramipexole was relatively low for safety, as described previously.

In conclusion, we demonstrated that pramipexole binds to D_2/D_3 receptors in the prefrontal cortex, amygdala, and medial and lateral thalamus. These regions have been indicated to have some relation to depression and may be part of the target sites where pramipexole exerts its antidepressive effects.

Acknowledgments

The authors are thankful to Ms. Hiroko Tsukinari and Mr. Kunpei Hayashi for their technical assistance.

Author Contributions

Conceived and designed the experiments: K. Ishibashi K. Ishii K. Ishiwata. Performed the experiments: K. Ishibashi K. Ishii KO K. Ishiwata. Analyzed the data: K. Ishibashi KO K. Ishiwat. Contributed reagents/materials/analysis tools: K. Ishibashi K. Ishii KO HM K. Ishiwata. Wrote the paper: K. Ishibashi K. Ishiwata. Discussed the results: K. Ishibashi K. Ishii KO HM K. Ishiwata.

References

1. Bennett JP, Jr., Piercey MF (1999) Pramipexole–a new dopamine agonist for the treatment of Parkinson's disease. J Neurol Sci 163: 25–31.
2. Lieberman A, Ranhosky A, Korts D (1997) Clinical evaluation of pramipexole in advanced Parkinson's disease: results of a double-blind, placebo-controlled, parallel-group study. Neurology 49: 162–168.
3. Shannon KM, Bennett JP, Jr., Friedman JH (1997) Efficacy of pramipexole, a novel dopamine agonist, as monotherapy in mild to moderate Parkinson's disease. The Pramipexole Study Group. Neurology 49: 724–728.
4. Barone P, Scarzella L, Marconi R, Antonini A, Morgante L, et al. (2006) Pramipexole versus sertraline in the treatment of depression in Parkinson's disease: a national multicenter parallel-group randomized study. J Neurol 253: 601–607.
5. Lemke MR, Brecht HM, Koester J, Kraus PH, Reichmann H (2005) Anhedonia, depression, and motor functioning in Parkinson's disease during treatment with pramipexole. J Neuropsychiatry Clin Neurosci 17: 214–220.
6. Reichmann H, Brecht MH, Koster J, Kraus PH, Lemke MR (2003) Pramipexole in routine clinical practice: a prospective observational trial in Parkinson's disease. CNS Drugs 17: 965–973.
7. Rektorova I, Rektor I, Bares M, Dostal V, Ehler E, et al. (2003) Pramipexole and pergolide in the treatment of depression in Parkinson's disease: a national multicentre prospective randomized study. Eur J Neurol 10: 399–406.
8. Lattanzi L, Dell'Osso L, Cassano P, Pini S, Rucci P, et al. (2002) Pramipexole in treatment-resistant depression: a 16-week naturalistic study. Bipolar Disord 4: 307–314.
9. Corrigan MH, Denahan AQ, Wright CE, Ragual RJ, Evans DL (2000) Comparison of pramipexole, fluoxetine, and placebo in patients with major depression. Depress Anxiety 11: 58–65.
10. Goldberg JF, Burdick KE, Endick CJ (2004) Preliminary randomized, double-blind, placebo-controlled trial of pramipexole added to mood stabilizers for treatment-resistant bipolar depression. Am J Psychiatry 161: 564–566.
11. Zarate CA, Jr., Payne JL, Singh J, Quiroz JA, Luckenbaugh DA, et al. (2004) Pramipexole for bipolar II depression: a placebo-controlled proof of concept study. Biol Psychiatry 56: 54–60.
12. DeBattista C, Solvason HB, Breen JA, Schatzberg AF (2000) Pramipexole augmentation of a selective serotonin reuptake inhibitor in the treatment of depression. J Clin Psychopharmacol 20: 274–275.
13. Ostow M (2002) Pramipexole for depression. Am J Psychiatry 159: 320–321.
14. Sporn J, Ghaemi SN, Sambur MR, Rankin MA, Recht J, et al. (2000) Pramipexole augmentation in the treatment of unipolar and bipolar depression: a retrospective chart review. Ann Clin Psychiatry 12: 137–140.
15. Perugi G, Toni C, Ruffolo G, Frare F, Akiskal H (2001) Adjunctive dopamine agonists in treatment-resistant bipolar II depression: an open case series. Pharmacopsychiatry 34: 137–141.
16. Cassano P, Lattanzi L, Soldani F, Navari S, Battistini G, et al. (2004) Pramipexole in treatment-resistant depression: an extended follow-up. Depress Anxiety 20: 131–138.
17. Maj J, Rogoz Z, Skuza G, Kolodziejczyk K (1997) The behavioural effects of pramipexole, a novel dopamine receptor agonist. Eur J Pharmacol 324: 31–37.
18. Willner P, Lappas S, Cheeta S, Muscat R (1994) Reversal of stress-induced anhedonia by the dopamine receptor agonist, pramipexole. Psychopharmacology (Berl) 115: 454–462.
19. Missale C, Nash SR, Robinson SW, Jaber M, Caron MG (1998) Dopamine receptors: from structure to function. Physiol Rev 78: 189–225.
20. Millan MJ, Maiofiss L, Cussac D, Audinot V, Boutin JA, et al. (2002) Differential actions of antiparkinson agents at multiple classes of monoaminergic receptor. I. A multivariate analysis of the binding profiles of 14 drugs at 21 native and cloned human receptor subtypes. J Pharmacol Exp Ther 303: 791–804.
21. Mierau J, Schneider FJ, Ensinger HA, Chio CL, Lajiness ME, et al. (1995) Pramipexole binding and activation of cloned and expressed dopamine D2, D3 and D4 receptors. Eur J Pharmacol 290: 29–36.
22. Piercey MF (1998) Pharmacology of pramipexole, a dopamine D3-preferring agonist useful in treating Parkinson's disease. Clin Neuropharmacol 21: 141–151.
23. Kvernmo T, Hartter S, Burger E (2006) A review of the receptor-binding and pharmacokinetic properties of dopamine agonists. Clin Ther 28: 1065–1078.

24. Gurevich EV, Joyce JN (1999) Distribution of dopamine D3 receptor expressing neurons in the human forebrain: comparison with D2 receptor expressing neurons. Neuropsychopharmacology 20: 60–80.
25. Murray AM, Ryoo HL, Gurevich E, Joyce JN (1994) Localization of dopamine D3 receptors to mesolimbic and D2 receptors to mesostriatal regions of human forebrain. Proc Natl Acad Sci U S A 91: 11271–11275.
26. Sokoloff P, Giros B, Martres MP, Bouthenet ML, Schwartz JC (1990) Molecular cloning and characterization of a novel dopamine receptor (D3) as a target for neuroleptics. Nature 347: 146–151.
27. Bouthenet ML, Souil E, Martres MP, Sokoloff P, Giros B, et al. (1991) Localization of dopamine D3 receptor mRNA in the rat brain using in situ hybridization histochemistry: comparison with dopamine D2 receptor mRNA. Brain Res 564: 203–219.
28. Landwehrmeyer B, Mengod G, Palacios JM (1993) Dopamine D3 receptor mRNA and binding sites in human brain. Brain Res Mol Brain Res 18: 187–192.
29. Diaz J, Pilon C, Le Foll B, Gros C, Triller A, et al. (2000) Dopamine D3 receptors expressed by all mesencephalic dopamine neurons. J Neurosci 20: 8677–8684.
30. Joyce JN (2001) Dopamine D3 receptor as a therapeutic target for antipsychotic and antiparkinsonian drugs. Pharmacol Ther 90: 231–259.
31. Levant B (1997) The D3 dopamine receptor: neurobiology and potential clinical relevance. Pharmacol Rev 49: 231–252.
32. Halldin C, Farde L, Hogberg T, Mohell N, Hall H, et al. (1995) Carbon-11-FLB 457: a radioligand for extrastriatal D2 dopamine receptors. J Nucl Med 36: 1275–1281.
33. Olsson H, Halldin C, Farde L (2004) Differentiation of extrastriatal dopamine D2 receptor density and affinity in the human brain using PET. Neuroimage 22: 794–803.
34. Suhara T, Sudo Y, Okauchi T, Maeda J, Kawabe K, et al. (1999) Extrastriatal dopamine D2 receptor density and affinity in the human brain measured by 3D PET. Int J Neuropsychopharmacol 2: 73–82.
35. Lammertsma AA, Hume SP (1996) Simplified reference tissue model for PET receptor studies. Neuroimage 4: 153–158.
36. Logan J, Fowler JS, Volkow ND, Wolf AP, Dewey SL, et al. (1990) Graphical analysis of reversible radioligand binding from time-activity measurements applied to [N-11C-methyl]-(-)-cocaine PET studies in human subjects. J Cereb Blood Flow Metab 10: 740–747.
37. Loc'h C, Halldin C, Bottlaender M, Swahn CG, Moresco RM, et al. (1996) Preparation of [76Br]FLB 457 and [76Br]FLB 463 for examination of striatal and extrastriatal dopamine D-2 receptors with PET. Nucl Med Biol 23: 813–819.
38. Nestler EJ, Carlezon WA, Jr. (2006) The mesolimbic dopamine reward circuit in depression. Biol Psychiatry 59: 1151–1159.
39. Di Chiara G, Loddo P, Tanda G (1999) Reciprocal changes in prefrontal and limbic dopamine responsiveness to aversive and rewarding stimuli after chronic mild stress: implications for the psychobiology of depression. Biol Psychiatry 46: 1624–1633.
40. Nikolaus S, Antke C, Muller HW (2009) In vivo imaging of synaptic function in the central nervous system: II. Mental and affective disorders. Behav Brain Res 204: 32–66.
41. Cabib S, Puglisi-Allegra S (1996) Stress, depression and the mesolimbic dopamine system. Psychopharmacology (Berl) 128: 331–342.
42. LeDoux JE (2000) Emotion circuits in the brain. Annu Rev Neurosci 23: 155–184.
43. Drevets WC (1998) Functional neuroimaging studies of depression: the anatomy of melancholia. Annu Rev Med 49: 341–361.
44. Remy P, Doder M, Lees A, Turjanski N, Brooks D (2005) Depression in Parkinson's disease: loss of dopamine and noradrenaline innervation in the limbic system. Brain 128: 1314–1322.
45. Espejo EF, Minano FJ (1999) Prefrontocortical dopamine depletion induces antidepressant-like effects in rats and alters the profile of desipramine during Porsolt's test. Neuroscience 88: 609–615.
46. Ohmori T, Arora RC, Meltzer HY (1992) Serotonergic measures in suicide brain: the concentration of 5-HIAA, HVA, and tryptophan in frontal cortex of suicide victims. Biol Psychiatry 32: 57–71.
47. Agren H, Reibring L, Hartvig P, Tedroff J, Bjurling P, et al. (1992) PET studies with L-[11C]5-HTP and L-[11C]dopa in brains of healthy volunteers and patients with major depression. Clin Neuropharmacol 15(Suppl 1 Pt A): 235A–236A.
48. Garcia-Cabezas MA, Rico B, Sanchez-Gonzalez MA, Cavada C (2007) Distribution of the dopamine innervation in the macaque and human thalamus. Neuroimage 34: 965–984.
49. Sanchez-Gonzalez MA, Garcia-Cabezas MA, Rico B, Cavada C (2005) The primate thalamus is a key target for brain dopamine. J Neurosci 25: 6076–6083.
50. Garcia-Cabezas MA, Martinez-Sanchez P, Sanchez-Gonzalez MA, Garzon M, Cavada C (2009) Dopamine innervation in the thalamus: monkey versus rat. Cereb Cortex 19: 424–434.
51. Vilkman H, Kajander J, Nagren K, Oikonen V, Syvalahti E, et al. (2000) Measurement of extrastriatal D2-like receptor binding with [11C]FLB 457–a test-retest analysis. Eur J Nucl Med 27: 1666–1673.
52. Olsson H, Halldin C, Swahn CG, Farde L (1999) Quantification of [11C]FLB 457 binding to extrastriatal dopamine receptors in the human brain. J Cereb Blood Flow Metab 19: 1164–1173.
53. Sudo Y, Suhara T, Inoue M, Ito H, Suzuki K, et al. (2001) Reproducibility of [11 C]FLB 457 binding in extrastriatal regions. Nucl Med Commun 22: 1215–1221.
54. Kaasinen V, Vilkman H, Hietala J, Nagren K, Helenius H, et al. (2000) Age-related dopamine D2/D3 receptor loss in extrastriatal regions of the human brain. Neurobiol Aging 21: 683–688.
55. Inoue M, Suhara T, Sudo Y, Okubo Y, Yasuno F, et al. (2001) Age-related reduction of extrastriatal dopamine D2 receptor measured by PET. Life Sci 69: 1079–1084.
56. De Lean A, Kilpatrick BF, Caron MG (1982) Dopamine receptor of the porcine anterior pituitary gland. Evidence for two affinity states discriminated by both agonists and antagonists. Mol Pharmacol 22: 290–297.
57. Sibley DR, De Lean A, Creese I (1982) Anterior pituitary dopamine receptors. Demonstration of interconvertible high and low affinity states of the D-2 dopamine receptor. J Biol Chem 257: 6351–6361.
58. George SR, Watanabe M, Di Paolo T, Falardeau P, Labrie F, et al. (1985) The functional state of the dopamine receptor in the anterior pituitary is in the high affinity form. Endocrinology 117: 690–697.
59. Seneca N, Finnema SJ, Farde L, Gulyas B, Wikstrom HV, et al. (2006) Effect of amphetamine on dopamine D2 receptor binding in nonhuman primate brain: a comparison of the agonist radioligand [11C]MNPA and antagonist [11C]raclopride. Synapse 59: 260–269.
60. Narendran R, Hwang DR, Slifstein M, Talbot PS, Erritzoe D, et al. (2004) In vivo vulnerability to competition by endogenous dopamine: comparison of the D2 receptor agonist radiotracer (-)-N-[11C]propyl-norapomorphine ([11C]NPA) with the D2 receptor antagonist radiotracer [11C]-raclopride. Synapse 52: 188–208.
61. Finnema SJ, Halldin C, Bang-Andersen B, Gulyas B, Bundgaard C, et al. (2009) Dopamine D(2/3) receptor occupancy of apomorphine in the nonhuman primate brain–a comparative PET study with [11C]raclopride and [11C]MNPA. Synapse 63: 378–389.
62. Peng T, Zysk J, Dorff P, Elmore CS, Strom P, et al. (2010) D2 receptor occupancy in conscious rat brain is not significantly distinguished with [(3)H]-MNPA, [(3)H]-(+)-PHNO, and [(3)H]-raclopride. Synapse 64: 624–633.
63. Asselin MC, Montgomery AJ, Grasby PM, Hume SP (2007) Quantification of PET studies with the very high-affinity dopamine D2/D3 receptor ligand [11C]FLB 457: re-evaluation of the validity of using a cerebellar reference region. J Cereb Blood Flow Metab 27: 378–392.

OPEN ACCESS Freely available online PLoS one

Adenosine A_{2A} Receptors Measured with [^{11}C]TMSX PET in the Striata of Parkinson's Disease Patients

Masahiro Mishina[1,2,3]*, Kiichi Ishiwata[1], Mika Naganawa[1,4], Yuichi Kimura[1,5], Shin Kitamura[2,6], Masahiko Suzuki[1,7], Masaya Hashimoto[1,7], Kenji Ishibashi[1,8], Keiichi Oda[1], Muneyuki Sakata[1], Makoto Hamamoto[2,3], Shiro Kobayashi[9], Yasuo Katayama[2], Kenji Ishii[1]

1 Positron Medical Center, Tokyo Metropolitan Institute of Gerontology, Itabashi-ku, Tokyo, Japan, **2** The Second Department of Internal Medicine, Nippon Medical School, Bunkyo-ku, Tokyo, Japan, **3** Department of Neurology, Nippon Medical School Chiba Hokusoh Hospital, Inzai-shi, Chiba, Japan, **4** Department of Diagnostic Radiology, PET Center, Yale University, New Haven, Connecticut, United States of America, **5** Biophysics Group, Molecular Imaging Center, National Institute of Radiological Sciences, Chiba, Japan, **6** Department of Internal Medicine, Nippon Medical School Musashi Kosugi Hospital, Kawasaki, Kanagawa, Japan, **7** Department of Neurology, The Jikei University School of Medicine, Minato-ku, Tokyo, Japan, **8** Department of Neurology and Neurological Science Graduate School, Tokyo Medical and Dental University, Tokyo, Japan, **9** Department of Neurosurgery, Nippon Medical School Chiba Hokusoh Hospital, Inzai-shi, Chiba, Japan

Abstract

Adenosine A_{2A} receptors (A2ARs) are thought to interact negatively with the dopamine D_2 receptor (D2R), so selective A2AR antagonists have attracted attention as novel treatments for Parkinson's disease (PD). However, no information about the receptor in living patients with PD is available. The purpose of this study was to investigate the relationship between A2ARs and the dopaminergic system in the striata of drug-naïve PD patients and PD patients with dyskinesia, and alteration of these receptors after antiparkinsonian therapy. We measured binding ability of striatal A2ARs using positron emission tomography (PET) with [7-methyl-^{11}C]-(*E*)-8-(3,4,5-trimethoxystyryl)-1,3,7-trimethylxanthine ([^{11}C]TMSX) in nine drug-naïve patients with PD, seven PD patients with mild dyskinesia and six elderly control subjects using PET. The patients and eight normal control subjects were also examined for binding ability of dopamine transporters and D2Rs. Seven of the drug-naïve patients underwent a second series of PET scans following therapy. We found that the distribution volume ratio of A2ARs in the putamen were larger in the dyskinesic patients than in the control subjects ($p<0.05$, Tukey-Kramer *post hoc* test). In the drug-naïve patients, the binding ability of the A2ARs in the putamen, but not in the head of caudate nucleus, was significantly lower on the more affected side than on the less affected side ($p<0.05$, paired *t*-test). In addition, the A2ARs were significantly increased after antiparkinsonian therapy in the bilateral putamen of the drug-naïve patients ($p<0.05$, paired *t*-test) but not in the bilateral head of caudate nucleus. Our study demonstrated that the A2ARs in the putamen were increased in the PD patients with dyskinesia, and also suggest that the A2ARs in the putamen compensate for the asymmetrical decrease of dopamine in drug-naïve PD patients and that antiparkinsonian therapy increases the A2ARs in the putamen. The A2ARs may play an important role in regulation of parkinsonism in PD.

Citation: Mishina M, Ishiwata K, Naganawa M, Kimura Y, Kitamura S, et al. (2011) Adenosine A_{2A} Receptors Measured with [^{11}C]TMSX PET in the Striata of Parkinson's Disease Patients. PLoS ONE 6(2): e17338. doi:10.1371/journal.pone.0017338

Editor: Rafael Linden, Universidade Federal do Rio de Janeiro, Brazil

Received November 8, 2010; **Accepted** January 29, 2011; **Published** February 28, 2011

Funding: This work was funded by Grants-in-Aid for Scientific Research (B) No. 16390348, (B) No. 20390334, (C) No. 17590901 and (C) No. 20591033 from the Japan Society for the Promotion of Science (http://www.jsps.go.jp/english/e-grants/grants.html). The funders had no role in study design, data collection and analysis, decision to publish, or preparation of the manuscript.

Competing Interests: The authors have declared that no competing interests exist.

* E-mail: mishina@nms.ac.jp

Introduction

Parkinson's disease (PD) is a progressive degenerative neurological disorder characterized clinically by resting tremor, bradykinesia, cogwheel rigidity, and postural instability [1]. These symptoms result primarily from the loss of dopaminergic neurons in the substantia nigra and can be reduced by levodopa, which replenishes dopamine, and dopamine agonists.

Adenosine is as an endogenous modulator of synaptic function in the central nervous system [2], and its effects are mediated by at least four receptor subtypes: A_1, A_{2A}, A_{2B}, and A_3 [3]. Adenosine A_1 receptors (A1Rs) are widely distributed throughout the entire brain, while adenosine A_{2A} receptors (A2ARs) are enriched in the basal ganglia [4,5]. The A2AR is known to stimulate adenylyl cyclase and interacts with the dopamine D_2 receptor (D2R) negatively at the level of second messengers and beyond [5]. The A1R is known to inhibit adenylyl cyclase.

Recently, A2AR antagonists have attracted attention as potential non-dopaminergic therapies for PD. For example, caffeine is a nonselective adenosine receptor antagonist and is known to reduce the risk of developing PD [6,7]. In addition, theophylline, which is also a nonselective adenosine receptor antagonist, was expected to be a promising agent for the treatment of PD [8]. However, findings from clinical trials of both caffeine and theophylline have been unimpressive [9,10]. The selective A2AR antagonists was developed as novel nondopaminergic agents for PD [11] and provides antiparkinsonian benefit without causing or worsening dyskinesia, which is one of the most inconvenient side effects of dopaminergic therapy [12]. A postmortem study reported that the density of A2AR binding

sites in PD was comparable to that found in the normal subjects, while the density in the basal ganglia was lower in patients with Huntington's chorea than in normal subjects [13]. However, another study using *in situ* hybridization and autoradiography suggested that A2ARs were involved in the development of dyskinesia following long-term levodopa therapy in PD [14]. Therefore, A2ARs may be involved in the appearance of the side effects of antiparkinsonian agents. Although the A2AR has attracted much attention in PD therapies, clinical evidence describing A2ARs in living PD patients, such as drug-naïve patients, is lacking.

We developed PET ligands for mapping adenosine receptors, and we successfully visualized A1Rs with [1-methyl-^{11}C]8-dicyclopropylmethyl-1-methyl-3-propylxanthine ([^{11}C]MPDX) [15,16] and A2ARs with [7-methyl-^{11}C]-(*E*)-8-(3,4,5-trimethoxystyryl)-1,3,7-trimethylxanthine ([^{11}C]TMSX, Fig. 1) [17,18,19,20]. [^{11}C]TMSX has a xanthine structure and is an analog of istradefylline. In addition, the specific binding of [^{11}C]TMSX to A2ARs was confirmed with a theophylline challenge [21]. We performed test-retest studies and optimized the kinetics for [^{11}C]TMSX PET in normal subjects, thus confirming good reproducibility of [^{11}C]TMSX PET in the putamen. In this study, we investigated A2ARs in the striata of drug-naïve PD patients and PD patients with dyskinesia, and alteration of A2ARs after antiparkinsonian therapy using [^{11}C]TMSX PET.

Results

Figure 2 shows representative PET images for normal subjects, a drug-naïve PD patient before and after anti-parkinsonian therapy, and a PD patinet with dyskinesia.

Group comparison

There was no significant difference with age among the three groups, i. e. the drug naïve PD patients (five men and four women, mean age 64.6±5.7 years, Table 1), the PD patients with dyskinesia (two men and five women, mean age 65.0±7.3 years, Table 2) and the normal subjects (three men and three women, mean age 60.7±8.5 years). Rate of female was slightly large in the patients with dyskinesia [22], although not significant. In the PD, duration of disease was longer in the patients with dyskinesia (11.1±7.2 years) than the drug naïve patients (2.0±1.2 years, $p<0.001$, unpaired *t*-test). There was no significant difference with the Unified Parkinson's Disease Rating Scale part III (UPDRS-III) between the drug naïve patients (17.7±13.2) and the patients with dyskinesia (12.6±11.2).

The distribution volume ratio (DVR) for [^{11}C]TMSX in the bilateral putamen of patients with dyskinesia was larger with that normal controls ($p<0.05$), although that of drug-naïve patients was comparable with that of normal controls (Table 3). In the head of the caudate nucleus, the DVR of patients with dyskinesia was alightly larger than that of other two groups, although not significant.

In both the bilateral putamen and the head of the caudate nucleus, the uptake ratio index (URI) of [^{11}C]2β-carbomethoxy-3β-(4-fluorophenyl) tropane ([^{11}C]CFT), a marker for presynaptic dopamine transporter (DAT), in the bilateral putamen was significantly lower in the drug-naïve patients and patients with dyskinesia than in the normal controls (Table 3). The URI of [^{11}C]raclopride ([^{11}C]RAC), a marker for postsynaptic D2R, in the bilateral striata was lower in the patients with dyskinesia than in the controls and drug-naïve patients (Table 3).

Asymmetry in drug-naïve state

When we examined the asymmetrical symptoms in the early phase of PD as they relate to the PET images, we found that the DVR for [^{11}C]TMSX in the putamen was significantly lower on the more affected side than on the less affected side in the PD patients (Table 4). In contrast, the head of the caudate nucleus showed no significant differences between the more affected side and the less affected side according to DVRs for [^{11}C]TMSX.

The URI for [^{11}C]CFT in the putamen was significantly lower on the more affected side than on the less affected side in the drug-naïve patients, and the URI for [^{11}C]RAC was significantly higher on the more affected side than on the less affected side (Table 4). In the head of the caudate nucleus, there was no significant difference between the more affected side and the less affected side in the URI for either [^{11}C]CFT or [^{11}C]RAC.

Figure 3 demonstrates the lack of significant correlation among the DVR for [^{11}C]TMSX, the URI for [^{11}C]CFT and the URI for [^{11}C]RAC in the bilateral striata of drug-naïve patients. Specifically, there was no significant correlation among the following variables; the DVR for [^{11}C]TMSX versus the URI for [^{11}C]CFT (Figure 3A and 3D), the DVR for [^{11}C]TMSX versus the URI for [^{11}C]RAC (Figure 3B and 3E), and the URI for [^{11}C]CFT versus the URI for [^{11}C]RAC (Figure 3C and 3F).

Post-therapeutic state

In the seven PD patients with follow-up studies, the DVR for [^{11}C]TMSX in the bilateral putamen was significantly increased in the post-therapeutic state relative to the drug-naïve state (Table 5). The URIs for both [^{11}C]CFT and [^{11}C]RAC in the bilateral

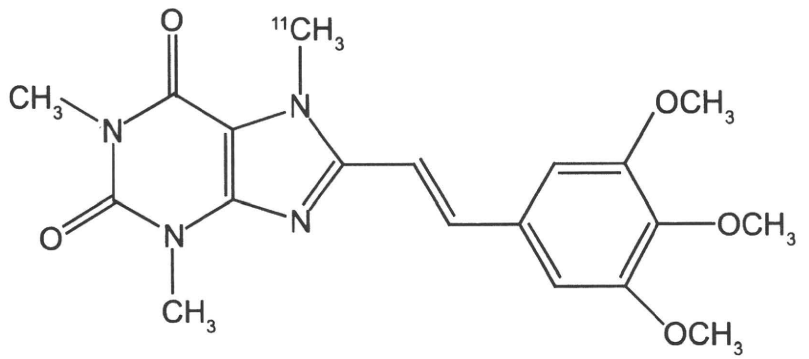

Figure 1. Structure of [^{11}C]TMSX.
doi:10.1371/journal.pone.0017338.g001

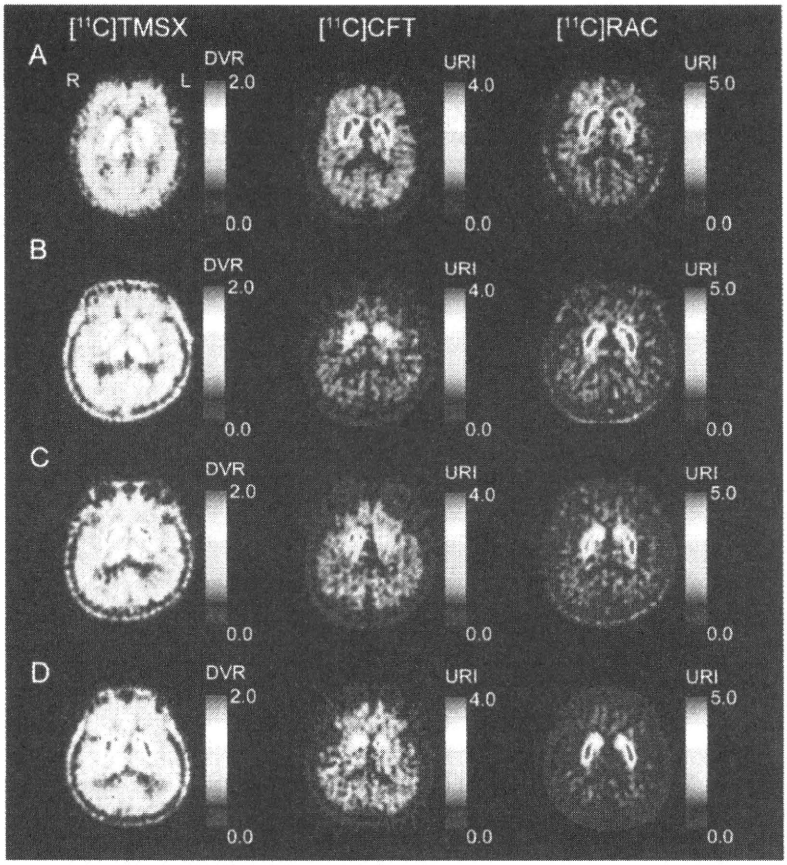

Figure 2. PET images for normal subjects, a drug-naïve patient with Parkinson's disease (PD), and a PD patient with dyskinesia. The normal subjects are a 63-year-old female for [^{11}C]TMSX, and a 63-year-old male for [^{11}C]CFT and [^{11}C]RAC (A). The drug-naïve patient is a 60-year-old male with right-dominant parkinsonism, and underwent two series of PET scans before (B) and after anti-parkinsonian therapy (C). The patients did not developed dyskinesia at a second series of PET scan in the post-therapeutic state. The DVR of [^{11}C]TMSX was smaller in the left putamen than in the right and was increased after treatment with anti-parkinsonian therapy for 14 months. The uptake of [^{11}C]CFT was reduced in the putamen, especially on the left. The uptake of [^{11}C]RAC was preserved in the striatum and was larger in the left putamen than in the right. The relative uptake of [^{11}C]CFT and [^{11}C]RAC in the putamen was lower in the post-therapeutic state than in the drug-naïve state. The PD patient with dyskinesia is a 65-year-old male with right-dominant parkinsonism (D). His disease duration was 19 years. The DVR of [^{11}C]TMSX was increased in the striata. The uptake of [^{11}C]CFT was significantly decreased in the putamen.
doi:10.1371/journal.pone.0017338.g002

putamen was significantly decreased in the post-therapeutic state than the drug-naïve state.

In the head of the caudate nucleus bilaterally, the URIs for [^{11}C]CFT and [^{11}C]RAC were significantly decreased in the post-therapeutic state than the drug-naïve state, but there was no significant difference in the DVR for [^{11}C]TMSX.

Discussion

As previous stidies reported [13,14,23], our PET study demonstrates that the putaminal binding ability of A2ARs was increased in the PD patients with dyskinesia, and that there was no significant difference in the striatal binding ability of A2ARs between drug-naïve PD patients and normal controls. However, in drawing attention to the asymmetrical symptoms in drug-naïve PD, our study suggests that A2ARs were asymmetrically down-regulated in the putamen but not in the head of the caudate nucleus. The function of A2ARs is thought to be opposite to that of D2Rs [5]. PET studies using [^{11}C]RAC have shown elevated binding of D2Rs in the putamen in early PD [24,25,26], due to decreased endogenous dopamine and weak D2R affinity for [^{11}C]RAC [27]. However, a postmortem study reported that the density of the D2R binding sites was higher in PD patients than normal controls [28]. Therefore, D2Rs are thought to be up-regulated in the putamen of the patients with advanced PD. Past studies indicated that 80% loss of dopaminergic neurons in the substantia nigra was needed to be developed to symptoms of PD, because such compensatory change of D2Rs is thought to delay the onset of symptoms of PD [29]. We reported on the asymmetrical compensation of the $sigma_1$ receptor for the reduction of dopamine in the putamen in early PD [30]. Our study in the drug-naïve state suggested that A2ARs might play an important role in inhibition of asymmetrical parkinsonism in PD along with D2Rs and $sigma_1$ receptors.

In the patients with PD, DATs in the putamen were reduced in the diskinesic patients relative to the drug-naïve patients, and reduced in the post-therapeutic state relative to the drug-naïve state. These findings were considered to reflect the progression of PD. The uptake of [^{11}C]RAC in the putamen was reduced in the diskinesic patietnts relative to the drug-naïve patients, and reduced

Table 1. Demographic and clinical data of drug-naïve patients with Parkinson's disease.

No	Age (years)	Gender	Duration from onset (years)	Symptom	Hoehn & Yahr	UPDRS-III Pre-therapy	Duration of therapy (month)	Antiparkinsonian agents at post-therapy PET	LED (mg)	UPDRS-III Post-therapy
1	72	F	2.0	R>L	1	5	7.0	Levodopa and carbidopa	100	19
2	60	M	1.3	R>L	2	8	14.2	Pramipexole and amantadine	75	6
3	58	F	3.0	R>L	4	41	15.9	Pramipexole, levodopa and carbidopa	450	25
4	68	F	0.5	R>L	2	23	15.9	Pramipexole, amantadine, levodopa and carbidopa	137.5	4
5	64	M	1.2	L>R	1	6	12.9	Pramipexole	150	7
6	56	M	0.7	L>R	2.5	10	20.8	Pramipexole and amantadine	200	21
7	68	M	3.0	L>R	3	18	14.7	Ropinirole, selegiline, droxidopa, levodopa and benserazide	825.5	21
8	71	M	4.0	R>L	1.5	12	-	-	-	-
9	64	F	2.0	L>R	2.5	36	-	-	-	-
Mean±SD	64.6±5.7		2.0±1.2		2.2±1.0	17.7±13.2	14.5±13.2		276.9±272.2	14.7±8.7

UPDRS-III; Unified Parkinson's Disease Rating Scale part III. LED; levodopa-equivalent dose.
doi:10.1371/journal.pone.0017338.t001

in the post-therapeutic state relative to the drug-naïve state. These findings are consistent with the compensatory change of D2Rs. We think that there are two possible reasons. First, [^{11}C]RAC may have competed with the D2R agonists and increased endogenous dopamine due to levodopa, thus decreasing the binding of [^{11}C]RAC to D2Rs. Second, the antiparkinsonian therapy may have abrogated the compensation of D2R due to the decrease in the dopamine. These factors can affect the binding of [^{11}C]RAC in the striata, and it is difficult to detect the up-regulation of D2R using [^{11}C]RAC PET in the patients with PD.

Striatal GABAergic medium spiny neurons (MSNs) represent more than 90% of striatal neurons, and A2ARs are highly

Table 2. Demographic and clinical data of dyskinesic patients with Parkinson's disease.

No	Age (years)	Gender	Duration from onset (years)	Symptom	Hoehn & Yahr	UPDRS-III	UPDRS-IV	Antiparkinsonian agents	LED (mg)
1	73	F	5	R>L	2	8	5	Pramipexole, Levodopa, carbidopa and entacapone	416.7
2	65	M	19	R>L	3	9	6	Cabergoline, trihexyphenidyl hydrochloride, droxidopa levodopa and carbidopa	667.0
3	66	F	10	R>L	3	7	5	Trihexyphenidyl hydrochloride, zonisamide, levodopa and benserazide hydrochloride	300.0
4	50	F	2	R>L	2	11	3	Pramipexole, levodopa and carbidopa	750.0
5	66	F	9	L>R	3	13	4	Pramipexole, levodopa and carbidopa	225.0
6	65	M	11	L>R	2	3	7	Pramipexole, cabergoline, amantadine, levodopa and carbidopa	983.5
7	70	F	22	L>R	4	37	9	Pramipexole, trihexyphenidyl hydrochloride, amantadine, levodopa and carbidopa	500.0
Mean±SD	65.0±7.3		11.1±7.2		2.7±0.8	12.6±11.2	5.6±2.0		548.9±267.7

UPDRS-III; Unified Parkinson's Disease Rating Scale part III. LED; levodopa-equivalent dose.
doi:10.1371/journal.pone.0017338.t002

Table 3. The DVRs for [^{11}C]TMSX and URIs for [^{11}C]CFT and [^{11}C]RAC in the striata of normal controls, drug-naïve patients with Parkinson's disease (PD) and PD patients with dyskinesia.

Radiopharmaceutical	Normal Control	Drug-naïve PD	PD with dyskinesia
Putamen			
[^{11}C]TMSX	1.47±0.11	1.48±0.10	1.58±0.15*
[^{11}C]CFT	2.67±0.49	1.14±0.33‡	0.65±0.24‡,††
[^{11}C]RAC	3.10±0.42	3.43±0.55	2.86±0.70**
Head of the caudate nucleus			
[^{11}C]TMSX	1.38±0.08	1.37±0.09	1.44±0.15
[^{11}C]CFT	2.52±0.54	1.83±0.35§	1.36±0.39‡,**
[^{11}C]RAC	2.70±0.48	2.50±0.37	1.84±0.49‡,§§

Values are mean ± SD (Drug-naïve PD: n = 9; PD with dyskinesia: n = 7; normal: n = 6 for [^{11}C]TMSX and n = 8 for [^{11}C]CFT and [^{11}C]RAC). Binding of [^{11}C]TMSX was evaluated as the distribution volume ratio (DVR) and binding of [^{11}C]CFT or [^{11}C]RAC was expressed as the uptake ratio index (URI).
*p<0.05 (vs normals),
**p<0.05 (vs drug-naïve),
†p<0.005 (vs normal),
††p<0.005 (vs drug-naïve PD),
§p<0.0005 (vs normal),
§§p<0.0005 (vs drug-naïve),
‡p<0.0001 (vs normal),
‡‡p<0.0001 (vs drug-naïve PD, Tukey-Kramer *post hoc* test).
doi:10.1371/journal.pone.0017338.t003

expressed in the striatopallidal MSNs (indirect pathway) but not in the striatonigral MSNs (direct pathway) [31,32]. Postmortem studies demonstrated dendritic atrophy of MSNs during advanced PD [33,34]. Therefore, an alteration in A2AR expression may be involved in the dendritic atrophy in the MSNs.

Our study showed that the binding of [^{11}C]TMSX to A2ARs was increased in the putamen in the PD patients with mild dyskinesia. A postmortem study suggested that the messenger ribonucleic acid (mRNA) of A2ARs and [^{3}H]SCH-58261-specific binding to A2ARs were increased in the putamen of PD patients with dyskinesia following long-term levodopa therapy [14]. Another study showed that mRNA levels for the A2ARs were elevated in the putamen of levodopa-treated MPTP monkeys compared with controls, although autoradiography with [^{3}H]SCH-58261 could not showed significant difference [23].

Table 4. The asymmetry in DVRs for [11C]TMSX and URIs for [11C]CFT and [11C]RAC in the striata of drug-naïve patients with Parkinson's disease.

Radiopharmaceutical	More affected side	Less affected side
Putamen		
[^{11}C]TMSX	1.46±0.11	1.50±0.10*
[^{11}C]CFT	0.98±0.30	1.29±0.29†
[^{11}C]RAC	3.59±0.53	3.27±0.56†
Head of the caudate nucleus		
[^{11}C]TMSX	1.38±0.10	1.36±0.08
[^{11}C]CFT	1.78±0.33	1.89±0.38
[^{11}C]RAC	2.52±0.37	2.47±0.39

Values are mean ± SD (PD: n = 9). Binding of [^{11}C]TMSX was evaluated as the distribution volume ratio (DVR) and binding of [^{11}C]CFT or [^{11}C]RAC was expressed as the uptake ratio index (URI).
*p<0.05,
†p<0.005 (paired t-test).
doi:10.1371/journal.pone.0017338.t004

Our study also showed that the binding of [^{11}C]TMSX was increased in the putamen after the antiparkinsonian therapy. The finding may reflect alteration in compensation for the decrease of dopamine in the patients with PD. The drug-naïve patients in this study did not develop dyskinesia by the time of second series of PET scans. Therefore, our study suggests that the increase in putaminal A2ARs after antiparkinsonian therapy preceded the development of dyskinesia in patients with PD. Dyskinesia may be involved in the additional gain of the A2ARs. We may predict the onset of dyskinesia using sequential [^{11}C]TMSX PET examination. Moreover, a recent study suggested that dyskinesia may involve not only A2ARs but also A1Rs [35]. Further PET studies with [^{11}C]MPDX and [^{11}C]TMSX will be needed to clarify this issue.

In conclusion, [^{11}C]TMSX PET demonstrated that the distribution of A2ARs was increased in the putamen in PD patients with dyskinesia. A2ARs was asymmetrically down-regulated in the putamen in drug-naïve patients with PD, and the asymmetrical regulation of A2ARs seems to be involved in compensation for the decrease in dopamine. Our study also showed that the A2ARs were increased in the putamen after antiparkinsonian therapy.

Materials and Methods

Subjects

We studied nine drug-naïve patients with PD. Table 1 summarizes the clinical profiles of the patients. All patients were right-handed. Their PD diagnoses were based on their medical histories, physical and neurological examinations, laboratory tests, and magnetic resonance imaging (MRI) studies, to rule out other diseases [1,36,37]. They had no medical histories of bronchial asthma and did not take theophylline regularly. To confirm early diagnosis of PD, each patient was also examined for DATs and D2Rs by PET using [^{11}C]CFT and [^{11}C]RAC, respectively. Specifically, we confirmed low binding of [^{11}C]CFT and normal or high uptake of [^{11}C]RAC in the putamen of all patients [38,39,40]. After PET examinations for drug naïve state, we also

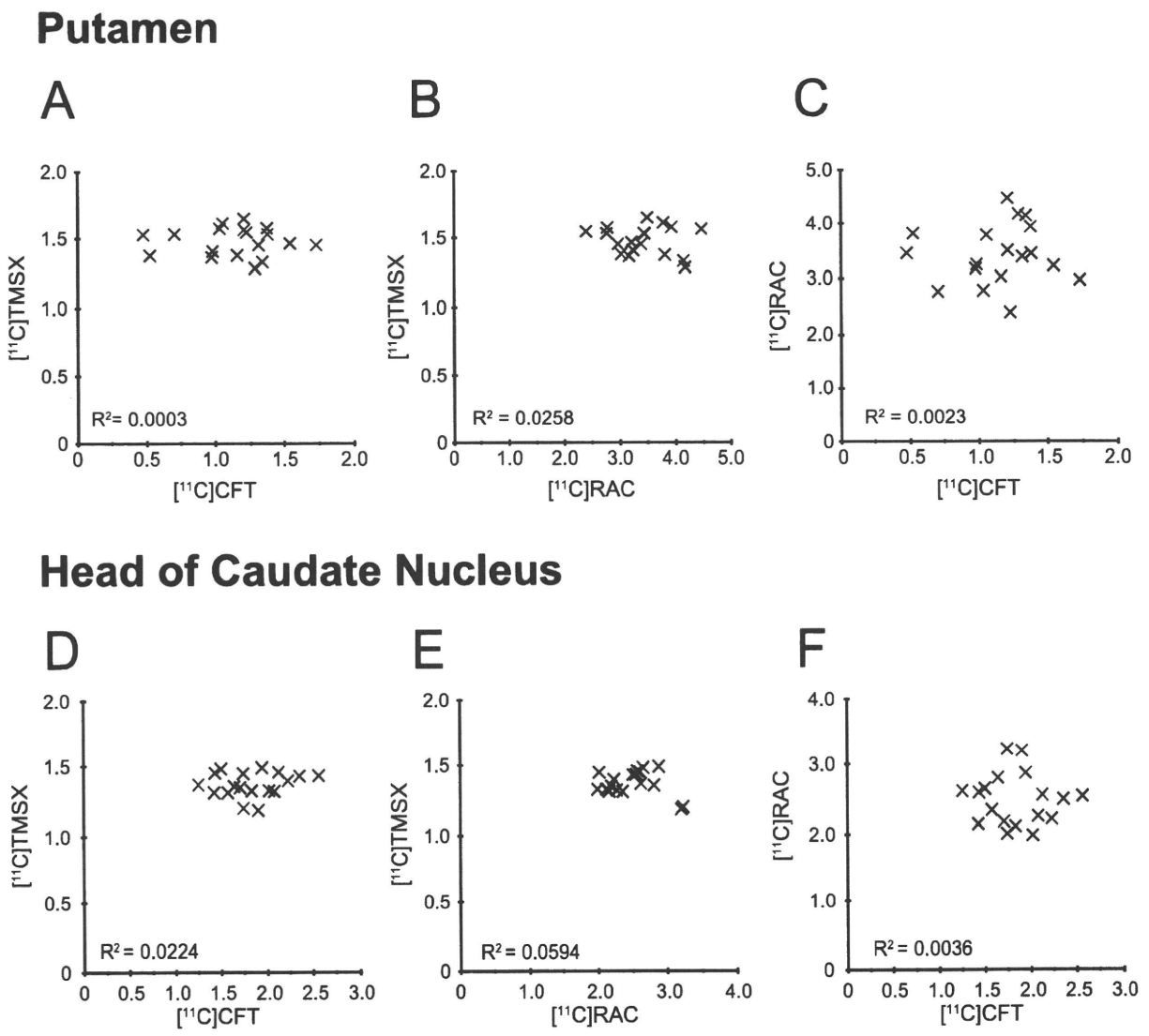

Figure 3. Scattergrams for binding parameters of [^{11}C]TMSX, [^{11}C]CFT and [^{11}C]RAC in the striata of drug-naïve patients. The binding parameter for [^{11}C]TMSX was expressed as DVR, and parameters for [^{11}C]CFT and [^{11}C]RAC were expressed as URI. There was no significant correlation among these variables.
doi:10.1371/journal.pone.0017338.g003

confirmed that the patients with PD were markedly ameliorated the parkinsonian symptoms by antiparkinsonian therapy, and that their diagnoses of PD remained unchanged in more than two years of observation. The patients did not experience hallucinations or dementia [41]. UPDRS-III was used to evaluate motor disability.

Seven of the nine patients were re-examined with [^{11}C]TMSX, [^{11}C]CFT and [^{11}C]RAC PET 14.5±4.1 months after starting antiparkinsonian therapy (Patients 1–7 in Table 1). The daily levodopa equivalent dose (LED) was calculated as follow: levodopa (mg) + levodopa (mg) ×1/3 (if on entacapone) + levodopa (mg) ×0.02× selegiline (mg) + pramipexole (mg) ×100 + ropinirole (mg) ×16.7 + cabergoline (mg) ×67 + pergolide (mg) ×100 + bromocriptine (mg) ×10. The LED for patients that underwent follow-up studies ranged from 75.0 to 825.5 mg (276.9±272.2 mg) at the time of post-therapeutic PET scanning. No patients developed dyskinesia during the period of this study. The administration of antiparkinsonian agents was not stopped before obtaining the PET scans at the therapeutic state.

We also studied advanced PD patients with mild dyskinesia. Table 2 summarizes the clinical profiles of the patients. All patients were right-handed. The LED for patients ranged from 225.0 to 983.5 mg (548.9±267.7 mg) at the time of PET scanning. The Unified Parkinson's Disease Rating Scale part IV (UPDRS-IV) was used to evaluate drug side effects such as dyskinesia. The dyskinesia of the patients was mild, and they could acquire PET examinations without any trouble caused by undesirable movements during the PET scanning.

For [^{11}C]TMSX PET scanning, the control group consisted of six volunteers. For [^{11}C]CFT and [^{11}C]RAC PET scanning, another control group was used, which consisted of eight volunteers (five men and three women, mean age ± SD, 62.3±6.9 years). The subjects in these control groups were all

Table 5. Therapeutic change in DVRs for [^{11}C]TMSX and URIs for [^{11}C]CFT and [^{11}C]RAC in the bilateral striata in the seven patients with Parkinson's disease.

Radiopharmaceutical	Drug-naïve state	Post-therapeutic state
Putamen		
[^{11}C]TMSX	1.46±0.12	1.50±0.09*
[^{11}C]CFT	1.12±0.36	0.88±0.23†
[^{11}C]RAC	3.44±0.42	2.76±0.78‡
Head of the caudate nucleus		
[^{11}C]TMSX	1.36±0.09	1.37±0.11
[^{11}C]CFT	1.74±0.29	1.48±0.23§
[^{11}C]RAC	2.56±0.37	2.01±0.52‡

Values are mean ± SD (n = 7). Binding of [^{11}C]TMSX was evaluated as the distribution volume ratio (DVR and binding of [^{11}C]CFT or [^{11}C]RAC was expressed as the uptake ratio index (URI).
*$p<0.05$,
†$p<0.005$,
§$p<0.001$,
‡$p<0.0005$ (paired t-test).
doi:10.1371/journal.pone.0017338.t005

right-handed. They did not have a history of neurological disease or any abnormalities on physical or neurological examinations. In addition, they did not take medications known to affect brain function and did not have a history of alcoholism. The normal subjects for [^{11}C]TMSX PET had no medical histories of bronchial asthma.

The study protocols were approved by the Ethics Committee of the Tokyo Metropolitan Institute of Gerontology. Written informed consent was obtained from all subjects who participated in this study.

[^{11}C]TMSX PET

PET was performed in the Tokyo Metropolitan Institute of Gerontology Positron Medical Center with an SET-2400W PET scanner (Shimadzu Co., Kyoto, Japan) [46]. Image manipulations were carried out on a MacBookPro computer with medical image processing software Dr. View/Linux R2.5 (AJS Inc., Tokyo, Japan) implemented in CentOS 5.4 (The CentOS Project, http://www.centos.org/) and Parallels Desktop 5 (Parallels Holdings, Ltd., Renton, WA, US).

All subjects avoided caffeine consumption over 12 hours before obtaining the [^{11}C]TMSX PET scans. The [^{11}C]TMSX was prepared as previously described [42]. Specific activity at the time of injection ranged from 40.6 to 119.5 GBq/μmol (69.6±20.8 GBq/μmol). After a transmission scan with a rotating ^{68}Ga/^{68}Ge line source to correct for the photon attenuation using the attenuation map, a dynamic series of decay-corrected PET data was acquired for 60 minutes using the 2D mode starting at the time of 700 MBq of [^{11}C]TMSX injection without arterial blood sampling. A total 27 of frames were taken, including six 10-s frames, three 30-s frames, five 1 min frames, five 2.5 min frames, and eight 5 min frames. All procedures for [^{11}C]TMSX PET scanning were performed under dim light to prevent photoisomerization of the [^{11}C]TMSX [42,43].

We generated early images for [^{11}C]TMSX PET by summing frames of the dynamic scan from 0 to 10 minutes [44], and we used these images as a reference for placing ROIs on the PET images of dynamic scans. We placed circular ROIs 10 mm in diameter on the PET images over the putamen and the head of the caudate nucleus bilaterally. In addition, we placed ROIs over the frontal lobe, temporal lobe, and occipital lobe to use as reference regions for kinetics analysis. We calculated regional time activity curves in the tissue (tTACs) from the dynamic data and ROIs, and we evaluated binding of [^{11}C]TMSX to A2ARs in the striata as a DVR using tTACs, a graphical analysis with the cerebral cortex as the reference region [45]. A kinetics analysis of the tTACs was performed using programs implemented in MATLAB version 7.04 (The Mathworks, Natick, MA, USA).

[^{11}C]CFT and [^{11}C]RAC PET

The [^{11}C]CFT was prepared as previously described [47]. The specific activity at the time of injection ranged from 10.3 to 300.3 GBq/μmol (51.9±60.1 GBq/μmol). Transmission data were acquired with a rotating ^{68}Ga/^{68}Ge rod source for attenuation correction. Each subject received an intravenous injection of 300 MBq of [^{11}C]CFT. Beginning 75 minutes after the injection, an emission scan was performed using the 3D mode, which lasted 15 minutes.

The [^{11}C]RAC was prepared as previously described [48]. The specific activity at the time of injection ranged from 5.7 to 280.0 GBq/μmol (63.1±57.4 GBq/μmol). Transmission data were acquired with a rotating ^{68}Ga/^{68}Ge rod source for attenuation correction. Each subject received an intravenous injection of 300 MBq of [^{11}C]RAC. Beginning 40 minutes after the injection, an emission scan was performed using the 3D mode, which lasted 15 minutes.

Circular regions of interest (ROIs) 10 mm in diameter were positioned on the PET images over the bilateral putamen, the head of the caudate nucleus and the cerebellar hemisphere. For a semi-quantitative analysis of the [^{11}C]CFT and [^{11}C]RAC PET, we calculated URI in the putamen and the head of the caudate nucleus [49] as follows:

$$URI = \frac{AS - AC}{AC}$$

where AS is the radioactivity in the ipsilateral putamen or the head of the caudate nucleus, and AC is the radioactivity of the bilateral cerebellar hemispheres.

Statistics

Among the drug naïve PD patients, the PD patients with dyskinesia and the normal subjects, One-way analysis of variance with Tukey-Kramer *post hoc* test were used to compare DVRs for [^{11}C]TMSX PET, URIs for [^{11}C]CFT and [^{11}C]RAC PET, and age. Where only two groups were compared, unpaired t test was used. Group difference in gender was calculated with the use of the chi-square test of proportions. In the drug naïve patients, striata from the more affected and the less affected side were compared, and the effect of therapeutic treatment on the striata was evaluated by the paired t-test. Regression analyses were used for comparison among binding parameters of [^{11}C]TMSX, [^{11}C]CFT and [^{11}C]RAC. The level of significance was set to $p<0.05$. Statistical values were computed using the software package JMP version 9.0.0 (SAS Institute Inc., Cary, NC, USA) on a Macintosh computer.

Acknowledgments

The authors thank Dr. T. Oda for the production of [^{11}C]TMSX and Ms. H. Tsukinari for caring for the subjects undergoing PET scanning.

Author Contributions

Conceived and designed the experiments: MM K. Ishiwata K. Ishii. Performed the experiments: MM K. Ishiwata M. Hashimoto K. Ishibashi KO K. Ishii. Analyzed the data: MM MN Y. Kimura M. Sakata. Contributed reagents/materials/analysis tools: MM K. Ishiwata MN S. Kitamura M. Suzuki M. Hashimoto K. Ishibashi KO M. Hamamoto S. Kobayashi Y. Katayama K. Ishii. Wrote the paper: MM K. Ishiwata MN Y. Kimura S. Kobayashi. Selection of subjects: S. Kitamura M. Suzuki M. Hashimoto K. Ishibashi K. Ishii.

References

1. Lees AJ, Hardy J, Revesz T (2009) Parkinson's disease. Lancet 373: 2055–2066.
2. Dunwiddie TV, Masino SA (2001) The role and regulation of adenosine in the central nervous system. Annu Rev Neurosci 24: 31–55.
3. Fredholm BB, AP IJ, Jacobson KA, Klotz KN, Linden J (2001) International Union of Pharmacology. XXV. Nomenclature and classification of adenosine receptors. Pharmacol Rev 53: 527–552.
4. Svenningsson P, Hall H, Sedvall G, Fredholm BB (1997) Distribution of adenosine receptors in the postmortem human brain: an extended autoradiographic study. Synapse 27: 322–335.
5. Fredholm BB, Svenningsson P (2003) Adenosine-dopamine interactions: development of a concept and some comments on therapeutic possibilities. Neurology 61: S5–9.
6. Ross GW, Abbott RD, Petrovitch H, Morens DM, Grandinetti A, et al. (2000) Association of coffee and caffeine intake with the risk of Parkinson disease. Jama 283: 2674–2679.
7. Ascherio A, Zhang SM, Hernan MA, Kawachi I, Colditz GA, et al. (2001) Prospective study of caffeine consumption and risk of Parkinson's disease in men and women. Ann Neurol 50: 56–63.
8. Kostic VS, Svetel M, Sternic N, Dragasevic N, Przedborski S (1999) Theophylline increases "on" time in advanced parkinsonian patients. Neurology 52: 1916.
9. Kulisevsky J, Barbanoj M, Gironell A, Antonijoan R, Casas M, et al. (2002) A double-blind crossover, placebo-controlled study of the adenosine A_{2A} antagonist theophylline in Parkinson's disease. Clin Neuropharmacol 25: 25–31.
10. Schwarzschild MA, Chen JF, Ascherio A (2002) Caffeinated clues and the promise of adenosine A_{2A} antagonists in PD. Neurology 58: 1154–1160.
11. Kase H (2001) New aspects of physiological and pathophysiological functions of adenosine A_{2A} receptor in basal ganglia. Biosci Biotechnol Biochem 65: 1447–1457.
12. Bara-Jimenez W, Sherzai A, Dimitrova T, Favit A, Bibbiani F, et al. (2003) Adenosine A_{2A} receptor antagonist treatment of Parkinson's disease. Neurology 61: 293–296.
13. Martinez-Mir MI, Probst A, Palacios JM (1991) Adenosine A_2 receptors: selective localization in the human basal ganglia and alterations with disease. Neuroscience 42: 697–706.
14. Calon F, Dridi M, Hornykiewicz O, Bedard PJ, Rajput AH, et al. (2004) Increased adenosine A_{2A} receptors in the brain of Parkinson's disease patients with dyskinesias. Brain 127: 1075–1084.
15. Fukumitsu N, Ishii K, Kimura Y, Oda K, Sasaki T, et al. (2003) Imaging of adenosine A_1 receptors in the human brain by positron emission tomography with [^{11}C]MPDX. Ann Nucl Med 17: 511–515.
16. Fukumitsu N, Ishii K, Kimura Y, Oda K, Sasaki T, et al. (2005) Adenosine A_1 receptor mapping of the human brain by PET with 8-dicyclopropylmethyl-1-^{11}C-methyl-3-propylxanthine. J Nucl Med 46: 32–37.
17. Ishiwata K, Kimura Y, Vries EFJd, Elsinga PH (2007) PET tracers for mapping adenosine receptors as probes for diagnosis of CNS disorders. CNS Agents Med Chem 7: 57–77.
18. Bauer A, Ishiwata K (2009) Adenosine receptor ligands and PET imaging of the CNS. Handb Exp Pharmacol. pp 617–642.
19. Ishiwata K, Kimura Y, Oda K, Ishii K, Sakata M, et al. (2010) Development of PET radiopharmaceuticals and their clinical applications at the Positron Medical Center. Geriatr Gerontol Int 10(Suppl 1): S180–196.
20. Mishina M, Ishiwata K, Kimura Y, Naganawa M, Oda K, et al. (2007) Evaluation of distribution of adenosine A_{2A} receptors in normal human brain measured with [^{11}C]TMSX PET. Synapse 61: 778–784.
21. Ishiwata K, Mishina M, Kimura Y, Oda K, Sasaki T, et al. (2005) First visualization of adenosine A_{2A} receptors in the human brain by positron emission tomography with [^{11}C]TMSX. Synapse 55: 133–136.
22. Zappia M, Annesi G, Nicoletti G, Arabia G, Annesi F, et al. (2005) Sex differences in clinical and genetic determinants of levodopa peak-dose dyskinesias in Parkinson disease: an exploratory study. Arch Neurol 62: 601–605.
23. Morissette M, Dridi M, Calon F, Tahar AH, Meltzer LT, et al. (2006) Prevention of dyskinesia by an NMDA receptor antagonist in MPTP monkeys: effect on adenosine A_{2A} receptors. Synapse 60: 239–250.
24. Antonini A, Schwarz J, Oertel WH, Beer HF, Madeja UD, et al. (1994) [^{11}C]raclopride and positron emission tomography in previously untreated patients with Parkinson's disease: Influence of L-dopa and lisuride therapy on striatal dopamine D2-receptors. Neurology 44: 1325–1329.
25. Rinne JO, Laihinen A, Ruottinen H, Ruotsalainen U, Nagren K, et al. (1995) Increased density of dopamine D_2 receptors in the putamen, but not in the caudate nucleus in early Parkinson's disease: a PET study with [^{11}C]raclopride. J Neurol Sci 132: 156–161.
26. Antonini A, Leenders KL, Vontobel P, Maguire RP, Missimer J, et al. (1997) Complementary PET studies of striatal neuronal function in the differential diagnosis between multiple system atrophy and Parkinson's disease. Brain 120(Pt 12): 2187–2195.
27. Ishibashi K, Ishii K, Oda K, Mizusawa H, Ishiwata K (2010) Competition between ^{11}C-raclopride and endogenous dopamine in Parkinson's disease. Nucl Med Commun 31: 159–166.
28. Piggott MA, Marshall EF, Thomas N, Lloyd S, Court JA, et al. (1999) Striatal dopaminergic markers in dementia with Lewy bodies, Alzheimer's and Parkinson's diseases: rostrocaudal distribution. Brain 122Pt 8: 1449–1468.
29. Jankovic J (2005) Progression of Parkinson disease: are we making progress in charting the course? Arch Neurol 62: 351–352.
30. Mishina M, Ishiwata K, Ishii K, Kitamura S, Kimura Y, et al. (2005) Function of sigma receptors in Parkinson's disease. Acta Neurol Scand 112: 103–107.
31. Mori A, Shindou T (2003) Modulation of GABAergic transmission in the striatopallidal system by adenosine A_{2A} receptors: a potential mechanism for the antiparkinsonian effects of A_{2A} antagonists. Neurology 61: S44–48.
32. Schiffmann SN, Jacobs O, Vanderhaeghen JJ (1991) Striatal restricted adenosine A_2 receptor (RDC8) is expressed by enkephalin but not by substance P neurons: an in situ hybridization histochemistry study. J Neurochem 57: 1062–1067.
33. McNeill TH, Brown SA, Rafols JA, Shoulson I (1988) Atrophy of medium spiny I striatal dendrites in advanced Parkinson's disease. Brain Res 455: 148–152.
34. Zaja-Milatovic S, Milatovic D, Schantz AM, Zhang J, Montine KS, et al. (2005) Dendritic degeneration in neostriatal medium spiny neurons in Parkinson disease. Neurology 64: 545–547.
35. Xiao D, Cassin JJ, Healy B, Burdett TC, Chen J-F, et al. (2010) Deletion of adenosine A_1 or A_{2A} receptors reduces L-3,4-dihydroxyphenylalanine-induced dyskinesia in a model of Parkinson's disease. Brain Res, in press.
36. Koller WC, Montgomery EB (1997) Issues in the early diagnosis of Parkinson's disease. Neurology 49: S10–25.
37. Gelb DJ, Oliver E, Gilman S (1999) Diagnostic criteria for Parkinson disease. Arch Neurol 56: 33–39.
38. Kaasinen V, Ruottinen HM, Nagren K, Lehikoinen P, Oikonen V, et al. (2000) Upregulation of putaminal dopamine D_2 receptors in early Parkinson's disease: a comparative PET study with [^{11}C] raclopride and [^{11}C]N-methylspiperone. J Nucl Med 41: 65–70.
39. Ribeiro MJ, Vidailhet M, Loc'h C, Dupel C, Nguyen JP, et al. (2002) Dopaminergic function and dopamine transporter binding assessed with positron emission tomography in Parkinson disease. Arch Neurol 59: 580–586.
40. Ishibashi K, Saito Y, Murayama S, Kanemaru K, Oda K, et al. (2010) Validation of cardiac ^{123}I-MIBG scintigraphy in patients with Parkinson's disease who were diagnosed with dopamine PET. Eur J Nucl Med Mol Imaging 37: 3–11.
41. McKeith IG, Dickson DW, Lowe J, Emre M, O'Brien JT, et al. (2005) Diagnosis and management of dementia with Lewy bodies: third report of the DLB Consortium. Neurology 65: 1863–1872.
42. Ishiwata K, Wang WF, Kimura Y, Kawamura K, Ishii K (2003) Preclinical studies on [^{11}C]TMSX for mapping adenosine A_{2A} receptors by positron emission tomography. Ann Nucl Med 17: 205–211.
43. Ishiwata K, Noguchi J, Wakabayashi S, Shimada J, Ogi N, et al. (2000) ^{11}C-labeled KF18446: a potential central nervous system adenosine A_{2A} receptor ligand. J Nucl Med 41: 345–354.
44. Mishina M, Senda M, Kimura Y, Toyama H, Ishiwata K, et al. (2000) Intrasubject correlation between static scan and distribution volume images for [^{11}C]flumazenil PET. Ann Nucl Med 14: 193–198.
45. Logan J, Fowler JS, Volkow ND, Wang GJ, Ding YS, et al. (1996) Distribution volume ratios without blood sampling from graphical analysis of PET data. J Cereb Blood Flow Metab 16: 834–840.
46. Fujiwara T, Watanuki S, Yamamoto S, Miyake M, Seo S, et al. (1997) Performance evaluation of a large axial field-of-view PET scanner: SET-2400W. Ann Nucl Med 11: 307–313.
47. Kawamura K, Oda K, Ishiwata K (2003) Age-related changes of the [^{11}C]CFT binding to the striatal dopamine transporters in the Fischer 344 rats: a PET study. Ann Nucl Med 17: 249–253.
48. Langer O, Dolle F, Lundkvist C, Sandell J, Swahn C, et al. (1999) Precursor synthesis and radiolabelling of the dopamine D_2 receptor ligand [^{11}C]raclopride from [^{11}C]methyl triflate. J Labelled Comp Radiopharm 42: 1183–1193.
49. Ishibashi K, Ishii K, Oda K, Kawasaki K, Mizusawa H, et al. (2009) Regional analysis of age-related decline in dopamine transporters and dopamine D_2-like receptors in human striatum. Synapse 63: 282–290.

J Neurol
DOI 10.1007/s00415-009-5377-y

LETTER TO THE EDITORS

Posterior cortical atrophy with [^{11}C] Pittsburgh compound B accumulation in the primary visual cortex

Taiki Kambe · Yumiko Motoi · Kenji Ishii · Nobutaka Hattori

Received: 24 August 2009 / Revised: 24 October 2009 / Accepted: 30 October 2009

Sirs,

Posterior cortical atrophy (PCA) is a presenile dementia that presents primarily with signs and symptoms of cortical visual dysfunction [1]. The most common associated pathologic findings of PCA are amyloid plaques and neurofibrillary tangles predominantly affecting the visual association areas [8]. Although [^{11}C] Pittsburgh compound B (PIB) PET studies of amnestic Alzheimer's disease (AD) have been conducted [2, 3, 5], the link between amyloid-β (Aβ) and regional brain dysfunction remains controversial. However, two PIB studies of PCA supported the possible link between Aβ deposition and clinical features [7, 10]. Here, we describe a patient with PCA who showed left homonymous hemianopsia and uncoupling between PIB uptake and glucose metabolism in the right occipital lobe.

A 63-year-old woman consulted our hospital with a 5-year history of poor vision. She first noticed that characters on posters appeared to be shaking. One year later, she found difficulty in reading subtitles in movies and then she became unable to read books. On neurological examination, she showed left homonymous hemianopsia. A Goldmann dynamic visual field examination demonstrated macular-sparing left homonymous hemianopsia. Visual acuity was normal and bilateral light reflexes were prompt. Other neurological examinations were normal. On neuropsychological evaluations, she showed visuospatial dysfunction and dyscalculia. MMSE score was 26 of 30. Memory function was preserved. She demonstrated disturbed recognition of superimposed figures. Face and color recognition were normal.

Cerebrospinal fluid (CSF) Aβ_{42} was decreased (297 pg/ml) and in normal controls, the levels are 874 $\pm$ 293 pg/ml (mean $\pm$ SD, INNOTEST® β-AMYLOID$_{(1\text{-}42)}$, Innogenetics, Ghent, Belgium). CSF tau protein phosphorylated at serine 199 was increased (1.36 pM). In normal controls, these levels are 0.6 $\pm$ 0.4 pM [4]. [^{18}F] fluorodeoxyglucose (FDG) PET image was acquired for 6 min starting 45 min after the injection of 150 MBq of tracer. The accumulation of [^{11}C] PIB was evaluated by a standardized uptake value ratio (SUVR) on a summing image obtained 40–60 min after injection of 500 MBq of tracer taking the cerebellar cortex as a reference region. [^{18}F] FDG PET showed hypometabolism in the temporo-parieto-occipital lobe predominantly on the right (Fig. 1d–f). [^{11}C] PIB PET demonstrated increased uptake in the bilateral frontal lobes and parietal and occipital cortices with more intense uptake on the right (Fig. 1g–i). In the right occipital lobe, FDG uptake showed lower metabolism in the lateral occipital cortex (Fig. 1d, e, arrow) than in the calcarine cortex (Fig. 1d, e, arrowhead). In contrast, amyloid imaging demonstrated high PIB uptake in the right calcarine cortex (Fig. 1g, h, arrowhead) while the adjacent lateral occipital cortex showed normal PIB uptake (Fig. 1g, h, arrow).

It was shown that macular sparing occurred when the posterior part of the calcarine cortex was spared in patients with striate cortical disease such as infarction, neoplasm and cerebromalacia, while macular splitting occurred when the occipital pole and operculum were involved [6]. Neuroimaging studies of our patient demonstrated that in the occipital lobe, there were two regions showing different

T. Kambe · Y. Motoi (✉) · N. Hattori
Department of Neurology,
Juntendo University School of Medicine,
2-1-1, Hongo Bunkyo-ku, Tokyo 113-8421, Japan
e-mail: motoi@juntendo.ac.jp

K. Ishii
Positron Medical Center,
Tokyo Metropolitan Institute of Gerontology,
1-1 Nakacho, Itabashi, Tokyo 173-0022, Japan

Published online: 14 November 2009

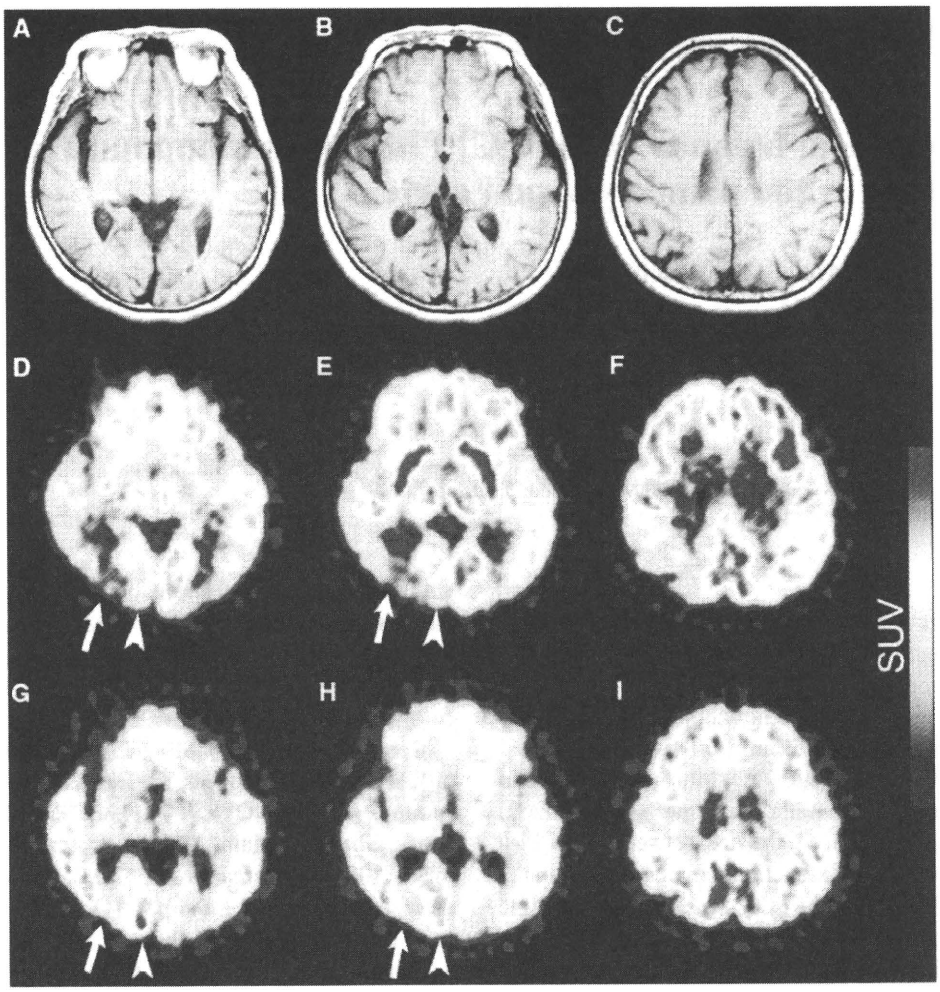

Fig. 1 Transverse T1-weighted MRI sections (**a–c**), PET with [^{18}F] FDG (D-F) and PET with [^{11}C] PIB (**g–i**) of the patient. MRI showed the absence of cerebral infarction and atrophy (**a**). The medial region including the calcarine cortex, (**d**, **e**, **g**, **h** *arrowhead*) showed moderately decreased FDG uptake and very high PIB uptake. In contrast, the lateral region demonstrated severely depressed FDG uptake without remarkable PIB uptake (**d**, **e**, **g**, **h**, *arrow*)

PIB/FDG patterns: a medial region (in the calcarine cortex, Fig. 1d, e, g, h arrowhead) with high PIB uptake and moderately decreased FDG uptake, and a lateral region with normal PIB uptake but severely depressed FDG uptake (Fig. 1d, e, g, h, arrow). Since PIB uptake in the medial region did not spare the occipital pole, we concluded that the lateral region is more likely to have contributed to the macular-sparing left hemianopsia.

We postulate that in the occipital lobe of our patient, Aβ deposition was not associated with the clinical features. Other factors such as neurofibrillary tangles might have contributed to the clinical features [9].

Acknowledgments We are grateful to Dr. Yoko Chikaoka for excellent technique regarding CSF analysis.

References

1. Benson DF, Davis RJ, Snyder BD (1988) Posterior cortical atrophy. Arch Neurol 45:789–793
2. Edison P, Archer HA, Hinz R, Hammers A, Pavese N, Tai YF, Hotton G, Cutler D, Fox N, Kennedy A, Rossor M, Brooks DJ (2007) Amyloid, hypometabolism, and cognition in Alzheimer disease: an [11C]PIB and [18F]FDG PET study. Neurology 68:501–508
3. Frisoni GB, Lorenzi M, Caroli A, Kemppainen N, Nagren K, Rinne JO (2009) In vivo mapping of amyloid toxicity in Alzheimer disease. Neurology 72:1504–1511
4. Itoh N, Arai H, Urakami K, Ishiguro K, Ohno H, Hampel H, Buerger K, Wiltfang J, Otto M, Kretzschmar H, Moeller HJ, Imagawa M, Kohno H, Nakashima K, Kuzuhara S, Sasaki H, Imahori K (2001) Large-scale, multicenter study of cerebrospinal fluid tau protein phosphorylated at serine 199 for the antemortem diagnosis of Alzheimer's disease. Ann Neurol 50:150–156